Using *in-silico* Models to Integrate *in-vitro* Data to Support Virtual Trials for Cost Effective Drug Development

November 5th, 2018

Viera Lukacova

Outline

- What is PBPK model?
- Parameterizing PBPK model using *in vitro* data
  - Dissolution & Precipitation
  - Passive Absorption
  - Pharmacokinetics
- Virtual Trials: Applications of calibrated PBPK model
- Summary

The Big Picture

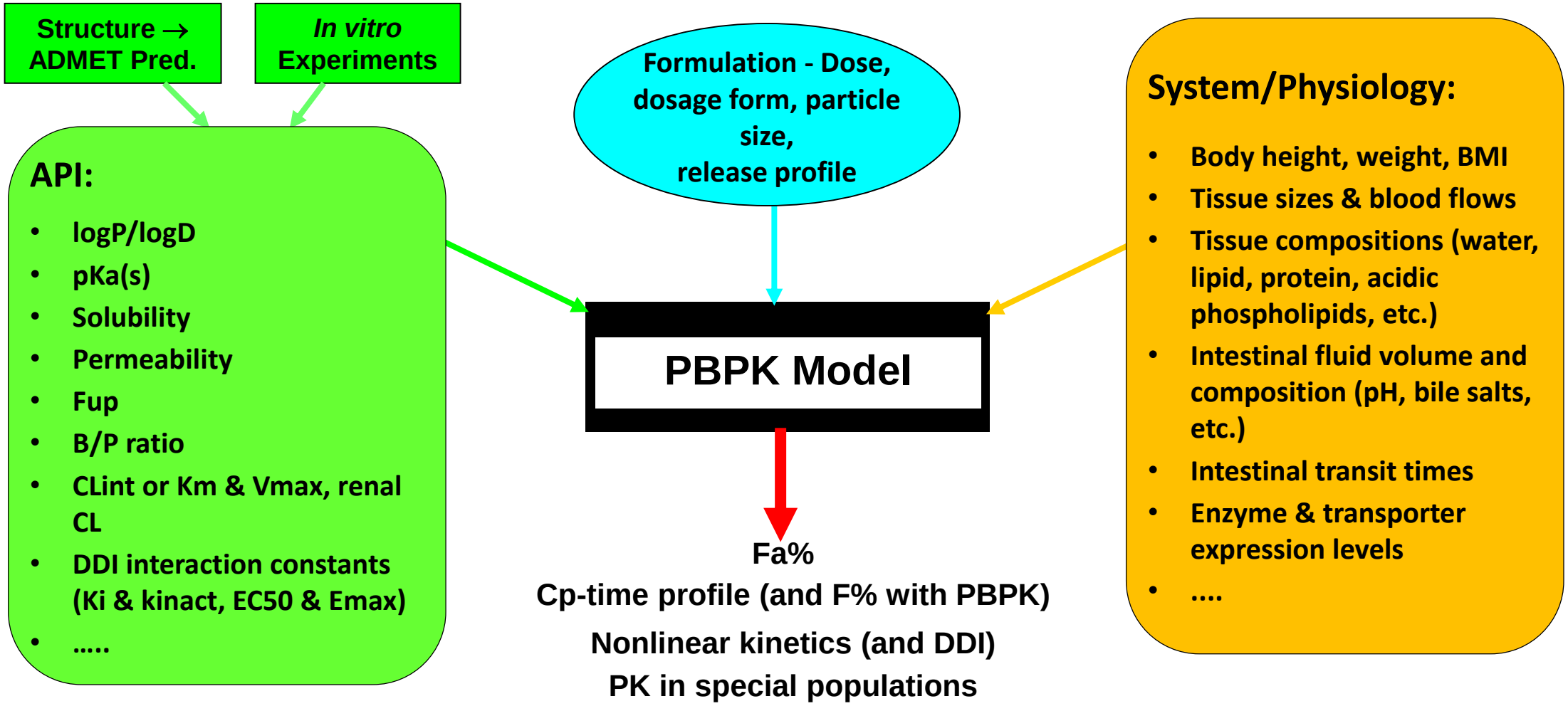

Advanced Compartmental Absorption and Transit Model (ACAT™)

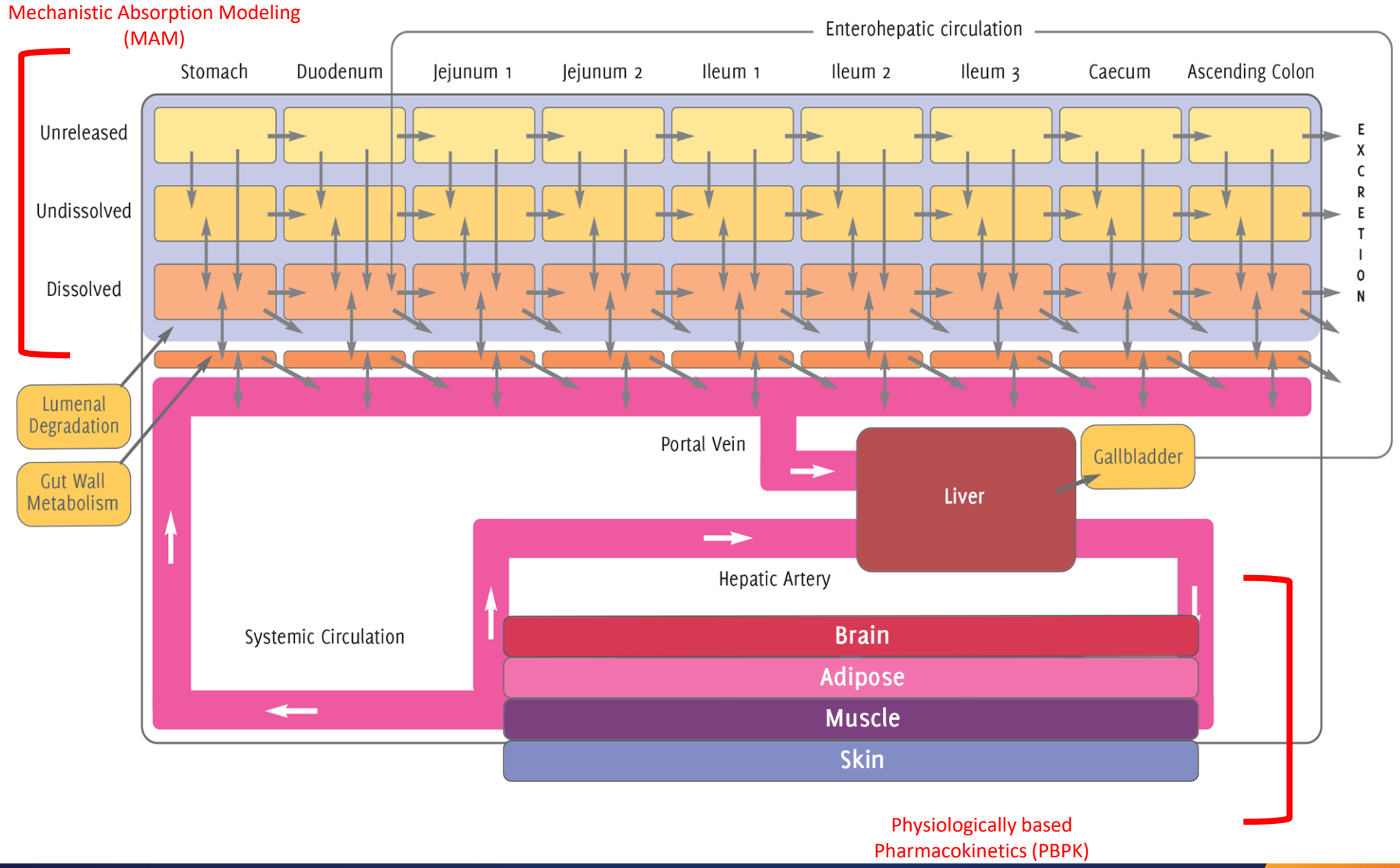

Discovery Preclinical Clinical

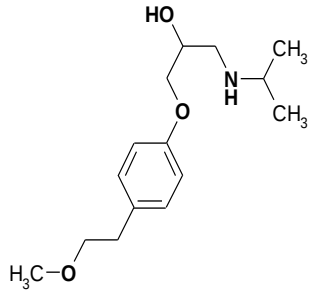

Discovery PK

Combine *in silico* technologies to screen compound libraries in animals or humans

Incorporate preclinical/*in vitro* data to extend FIH simulations to full *in vivo* outcomes (IVIVE)

Identify toxic dose levels in preclinical species

Clinical PK/Pharmacology

Simulate population behaviors (e.g., pediatrics, disease)

Build PBPK-PD models

Predict DDIs

Pharmaceutical Development

Assess various strategies during formulation development

Assist with Quality by Design (QbD) implementation

Develop mechanistic *in vitro-in vivo* correlations (IVIVCs)

Understand food effects

What is happening *in vivo* (oral administration)?

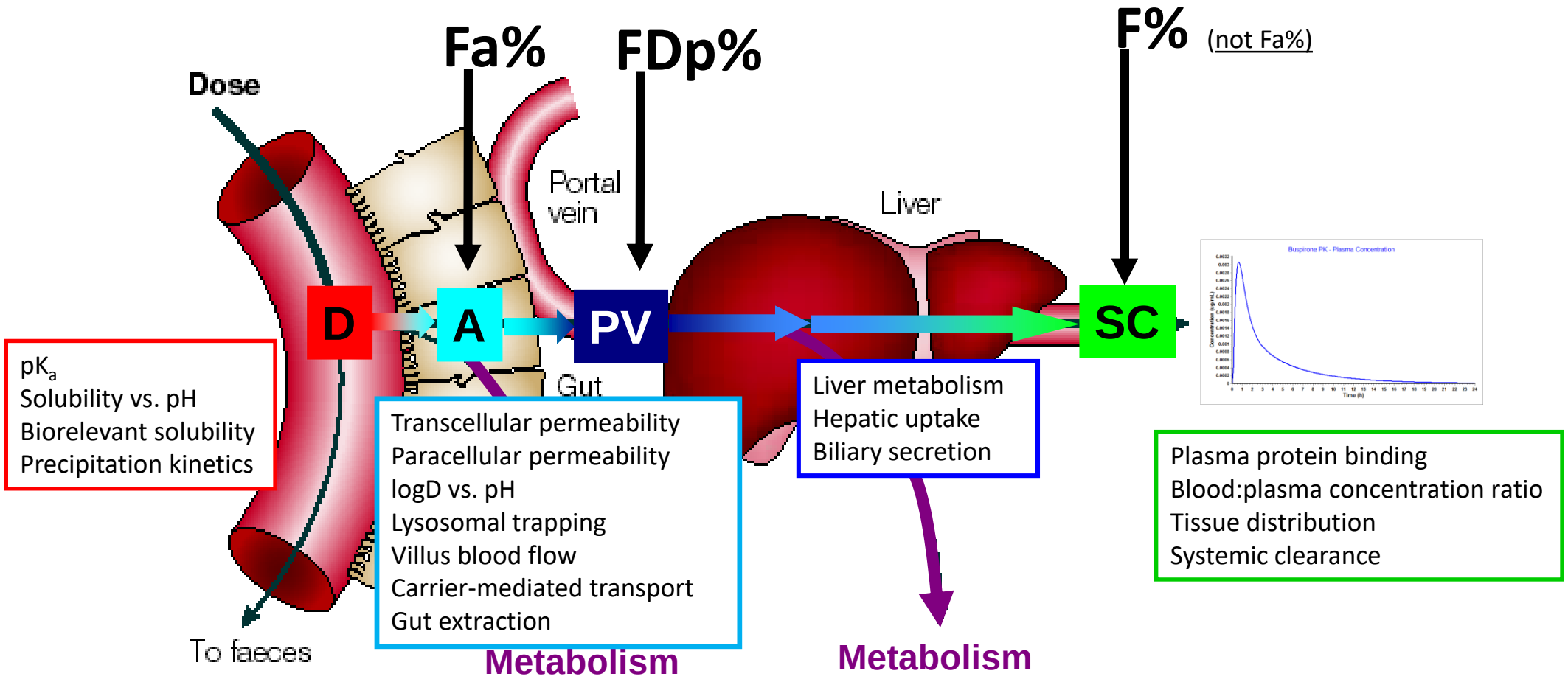

* Modified from van de Waterbeemd, H, and Gifford, E. *ADMET In Silico Modelling: Towards Prediction Paradise?* Nat. Rev. Drug Disc. 2003, 2:192-204

Solubility and Dissolution

Solubility

Changes in ionization result in changes in solubility in different regions of the intestine

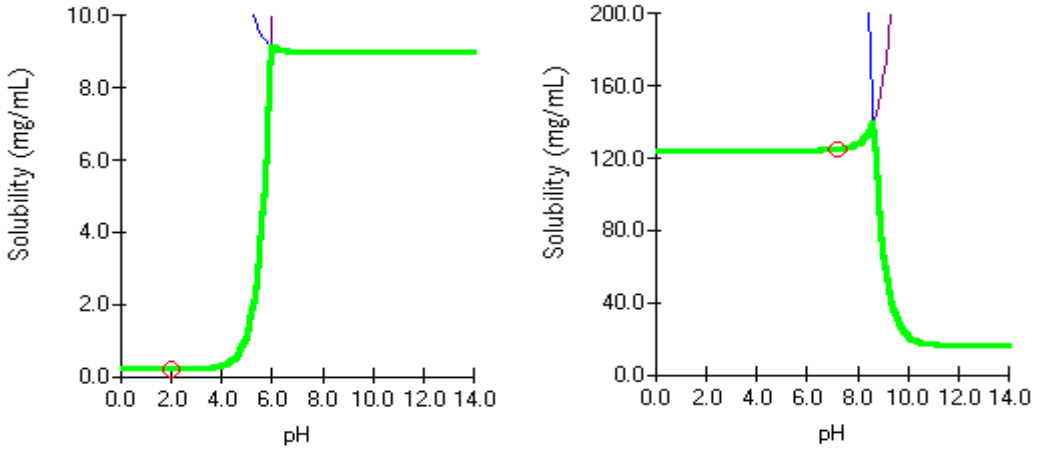

Changes in bile salt concentrations in different regions of the intestine may result in changes in solubility (especially for more lipophilic compounds)

$$Sol_{bile,pH} = Sol_{aq,pH}\left(1+\frac{MWt_{H_2O}}{\rho_{H_2O}}\times SR\times C_{bile}\right)$$

Mithani, Pharm Res 1996, 13:163-167

pH and bile salt concentrations

fasted:

Compartment Data		
Compartment	pH	Bile Salt (mM)
Stomach	1.30	0.0
Duodenum	6.00	2.800
Jejunum 1	6.20	2.330
Jejunum 2	6.40	2.030
Ileum 1	6.60	1.410
Ileum 2	6.90	1.160
Ileum 3	7.40	0.140
Caecum	6.40	0.0
Asc Colon	6.80	0.0

human:

Compartment Data		
Compartment	pH	Bile Salt (mM)
Stomach	3.90	0.0
Duodenum	5.89	20.00
Jejunum 1	6.13	17.29
Jejunum 2	6.13	6.980
Ileum 1	5.93	2.820
Ileum 2	5.93	1.300
Ileum 3	5.93	1.240
Caecum	6.58	0.0
Asc Colon	6.23	0.0

rat:

Compartment Data		
Compartment	pH	Bile Salt (mM)
Stomach	3.00	0.0
Duodenum	6.20	5.000
Jejunum 1	6.20	4.050
Jejunum 2	6.20	1.820
Ileum 1	6.40	0.610
Ileum 2	6.60	0.440
Ileum 3	6.68	0.310
Caecum	6.75	0.0
Asc Colon	6.45	0.0

dog:

fed:

Compartment Data		
Compartment	pH	Bile Salt (mM)
Stomach	4.90	0.0
Duodenum	5.40	14.44
Jejunum 1	5.40	12.02
Jejunum 2	6.00	10.46
Ileum 1	6.60	7.280
Ileum 2	6.90	5.990
Ileum 3	7.40	0.730
Caecum	6.40	0.0
Asc Colon	6.80	0.0

Compartment Data		
Compartment	pH	Bile Salt (mM)
Stomach	3.20	0.0
Duodenum	5.00	20.00
Jejunum 1	5.10	17.29
Jejunum 2	5.10	6.980
Ileum 1	5.94	2.820
Ileum 2	5.94	1.300
Ileum 3	5.94	1.240
Caecum	5.90	0.0
Asc Colon	5.51	0.0

Compartment Data		
Compartment	pH	Bile Salt (mM)
Stomach	5.00	0.0
Duodenum	6.20	15.40
Jejunum 1	6.20	12.50
Jejunum 2	6.20	5.600
Ileum 1	6.40	1.900
Ileum 2	6.60	1.340
Ileum 3	7.05	0.950
Caecum	7.50	0.0
Asc Colon	6.45	0.0

Dissolution

Dissolution rate coefficient (not a constant because it changes at every time step) in intestinal lumen compartment number *i* for particle size bin *j:*

$$\frac{dM_D}{dt} = \frac{D_w}{\rho r_t T}\frac{(1+2s)}{s}(C_s - C_l)M_{u,t}$$

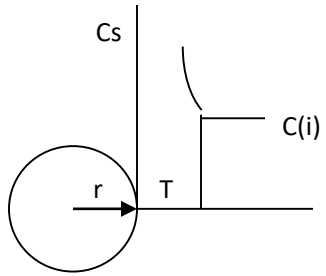

$T = r_{0j}$

D = diffusion coefficient

C_S = solubility at *local* pH

$C_{(i)}$ = lumen concentration in compartment *i*

ρ = particle density (***density of API crystals***)

r_j = spherical particle *radius* for particle size bin *j*

T = diffusion layer thickness (= particle radius up to a limit)

s = shape factor (***Length/diameter****) **–** for spherical particles = 1

*in the original Johnson equation, *s'=Length/radius* and the term is $\frac{2(1+s')}{s'}$

Predicting *in vivo* dissolution: Particle Size Distribution

$$\frac{dM_D}{dt} = \frac{D_w}{\rho r_t T}\frac{(1+2s)}{s}(C_s - C_l)M_{u,t}$$

Lu, Pharm Res 1993, 10:1308-1314

In vivo dissolution rate and extent is calculated from particle size distribution for each formulation and *in vivo* drug solubility (*in vivo* drug solubility is changing to account for changes in pH and bile salt concentration as the drug is moving through the intestine).

The model is applicable when API properties (solubility, particle size) drive the dissolution rate.

Prediction of *in vivo* performance for 3 cilostazol formulations with different API particle size distributions administered in dog

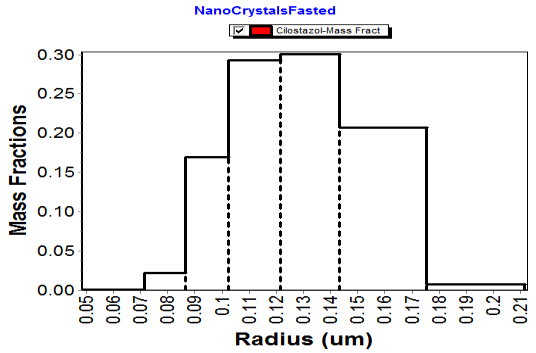

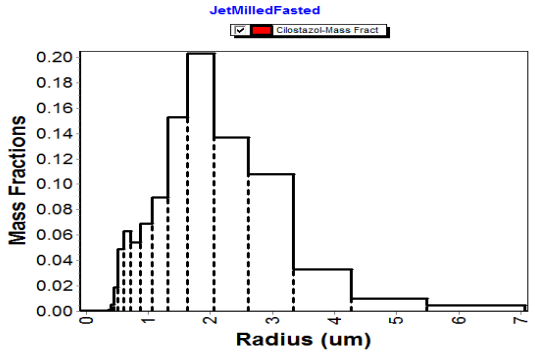

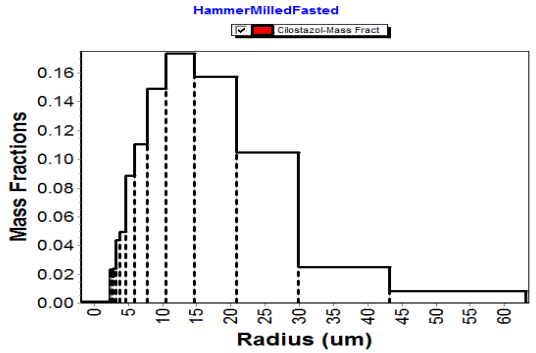

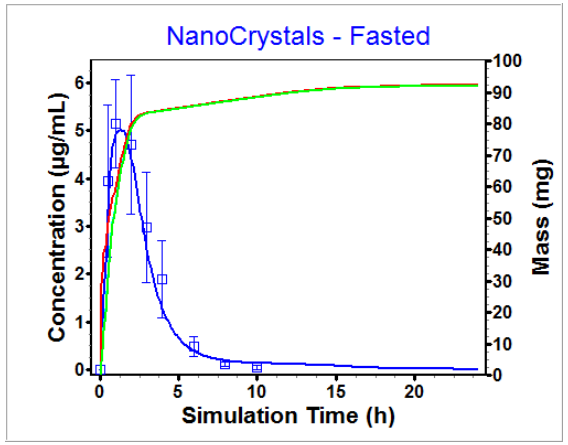

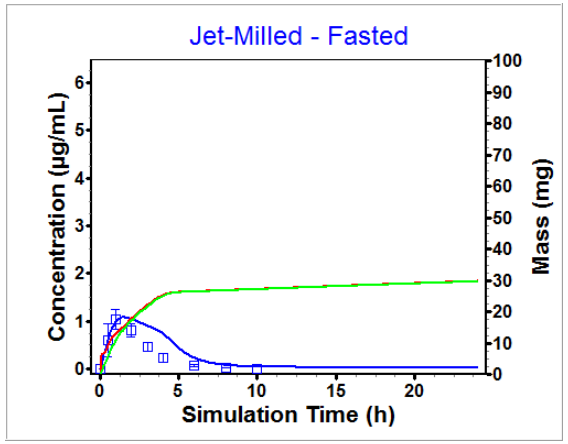

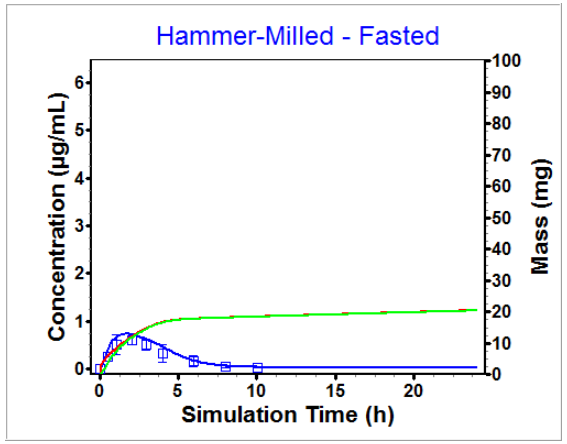

Observed data from Jinno, J Contr Rel 2006, 111: 56-64

Simulation results from GastroPlus v9.0

Predicting *in vivo* dissolution: z-factor

$$\frac{dM_D}{dt} = Z(C_s - C_l)M_{u,t}$$

Takano, Pharm Res 2006, 23:1144-1156

Z represents $\frac{3D_w}{\rho r T}$ and is determined by fitting to *in vitro* dissolution data.

In vivo dissolution rate and extent is calculated from z-factor fitted to *in vitro* dissolution profile for each formulation and *in vivo* drug solubility (*in vivo* drug solubility is changing to account for changes in pH and bile salt concentration as the drug is moving through the intestine)

The model is applicable when API properties or formulation (i.e. excipients) drive the dissolution rate.

Prediction of *in vivo* performance for 3 cilostazol formulations with different API particle size distributions administered in dog

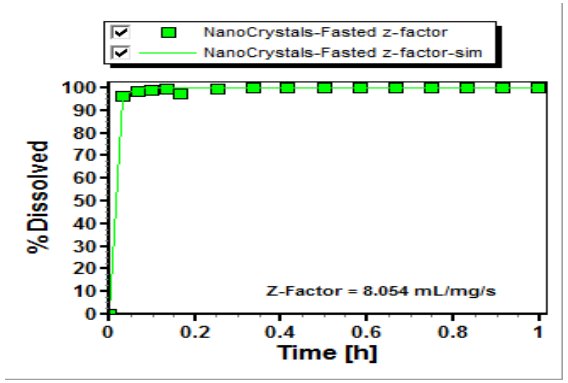

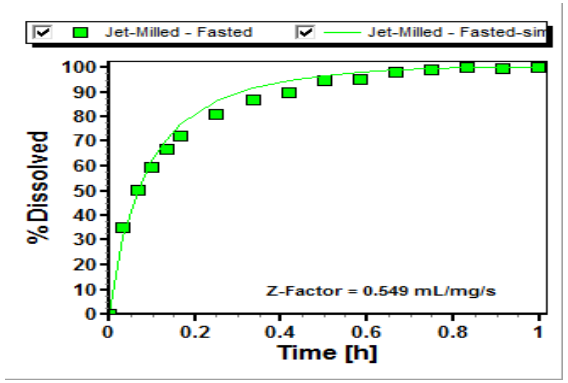

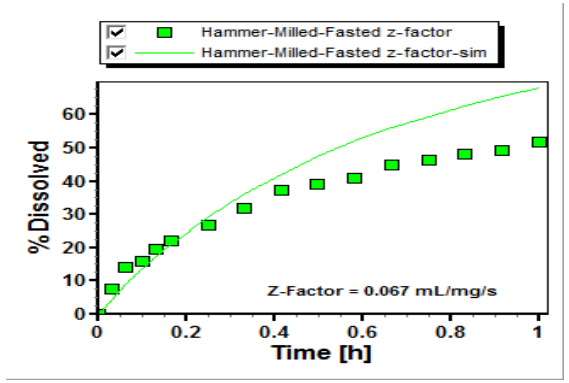

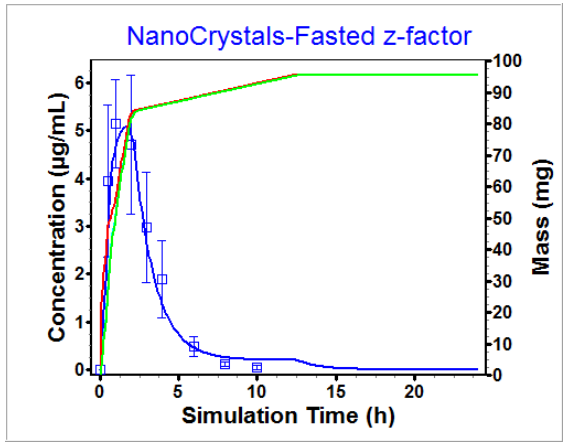

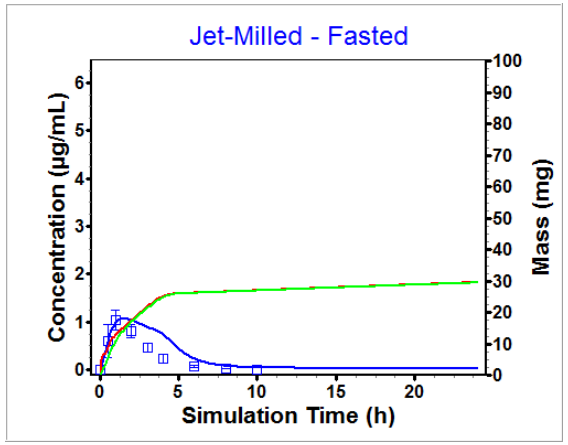

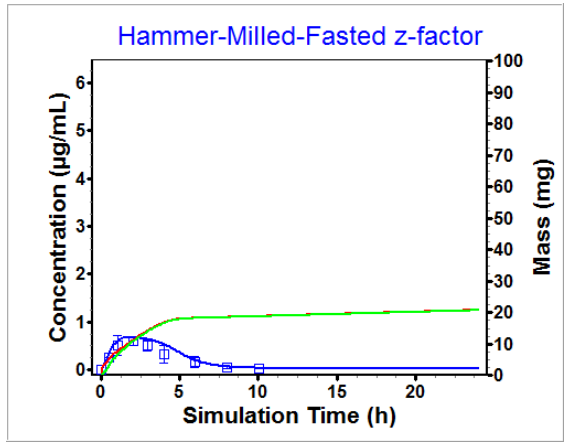

Observed data from Jinno, J Contr Rel 2006, 111: 56-64

Simulation results from GastroPlus v9.0

Predicting *in vivo* dissolution: Equivalent Particle Size

Theoretical particle size distribution was fitted to *in vitro* dissolution data and subsequently used as an in put in *in vivo* simulation

The model is applicable when formulation (i.e. excipients) drive the dissolution rate.

The *in vitro* dissolution profiles showed multi-phasic behavior for these formulation and could not be successfully fitted with single z-factor. Fitting artificial particle size distribution allowed for more accurate translation of *in vitro* dissolution to *in vivo*

Pepin et al. Mol Pharmaceutics 2016, 13:3256-3269

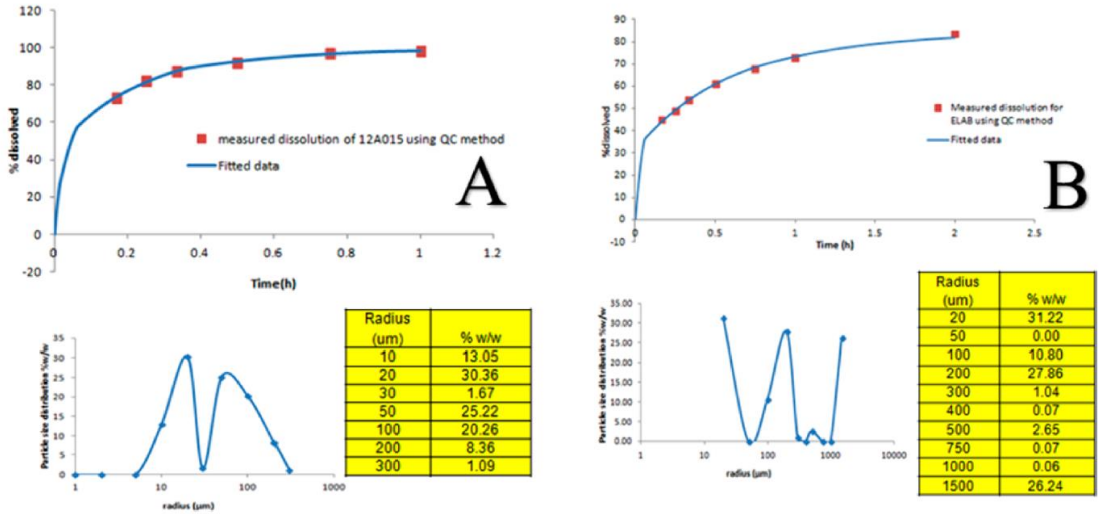

Radius (um)	% w/w
10	13.05
20	30.36
30	1.67
50	25.22
100	20.26
200	8.36
300	1.09

Radius (um)	% w/w
20	31.22
50	0.00
100	10.80
200	27.86
300	1.04
400	0.07
500	2.65
750	0.07
1000	0.06
1500	26.24

Figure 4. Fitting of dissolution profile for batch 12A015 (A) and ELAB (B) in the QC dissolution method with a theoretical particle size distribution. Note: the value presented at the 2 h time point for batch ELAB is from an infinity spin (15 min, 250 rpm).

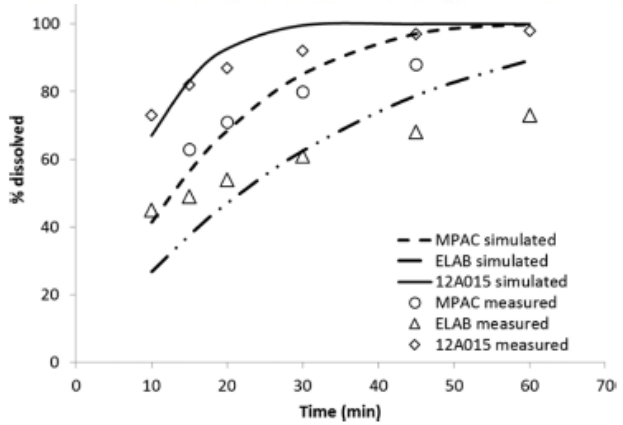

Figure 8. Z-factor fit for batches 12A015 ($Z = 1 \times 10^{-3}$ mL/mg/s), ELAB ($Z = 3.74 \times 10^{-4}$ mL/mg/s), and MPAC (Z = 5e-4 mL/mg/s).

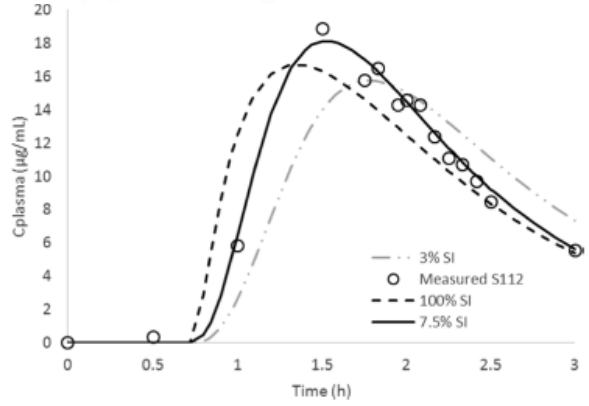

Figure 7. Simulated PK profile vs measured plasma concentrations for S112 following administration of 400 mg 12A015 tablet using Option A.

Precipitation

Enabled Formulation Strategies: BCS II

- Supersaturating Drug Delivery Systems
  - Salts
  - Cocrystals
  - Solutions
    - Lipidic formulations
    - Cyclodextrin complexes
    - Self (Micro) Emulsifying Drug Delivery Systems (S(M)EDDS)
  - Nanosuspensions (Stabilized)
  - Solid Dispersions (amorphous)

Supersaturating Drug Delivery Systems

Schematic diagram of “Spring and Parachute”

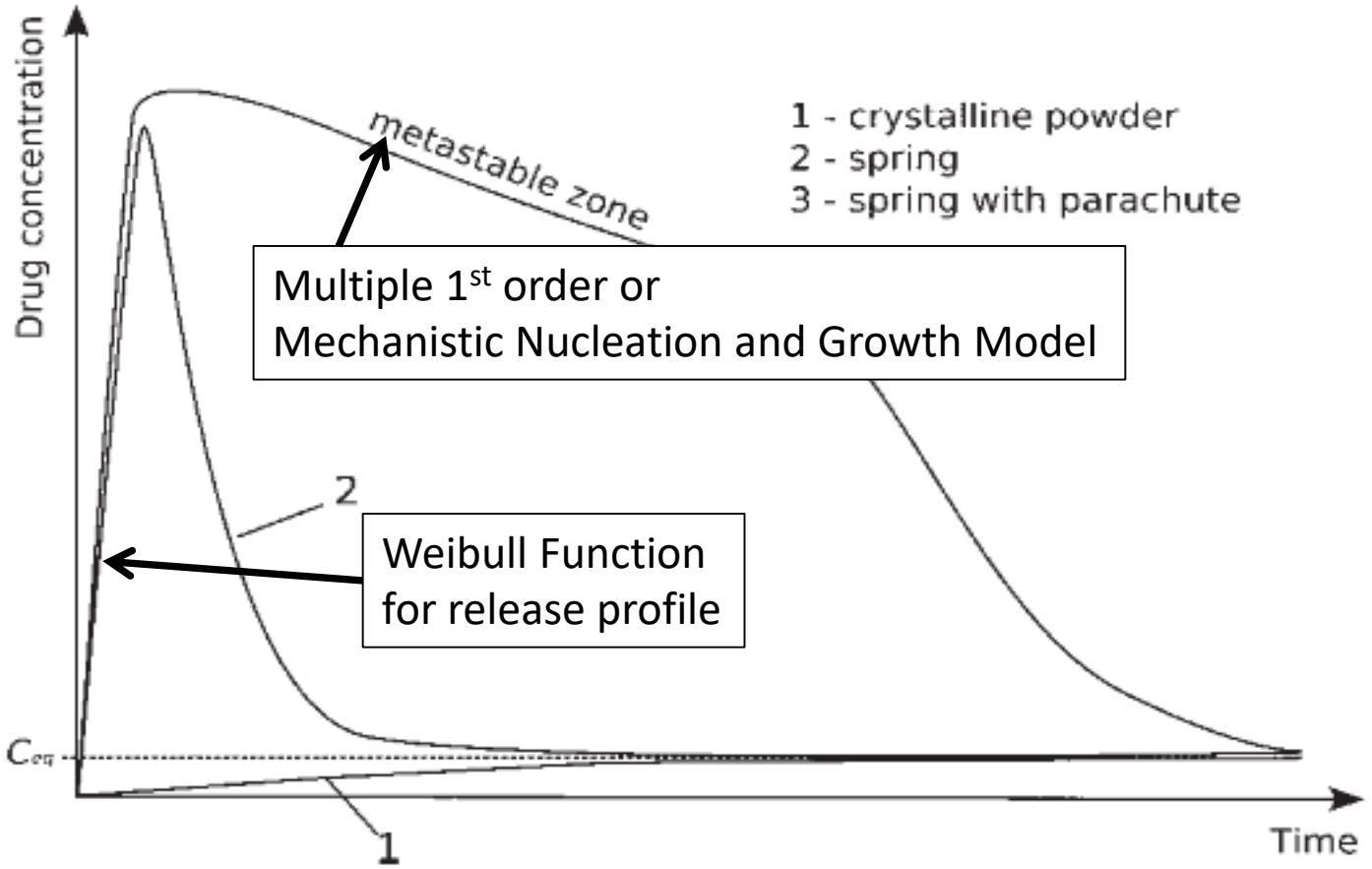

Brouwers J, J. Pharm. Sci. 98(8):2549 (2009)

Mechanistic Nucleation Theory

D_{mono}	Diffusion coefficient of the monomer (XXE-4 cm^2/min)
N_A	Avogadro's number (6.02E+23 molecs/mole)
c	Conc. of free monomer (moles/cm^3)
S	Solubility at the current pH
k_b	Boltzman's constant (1.38E-21 cJoules/Deg. K) (Note: Joule = Newton-meter)
T	310^o K
γ	Interfacial tension (Newtons/cm)
ν_m	Molecular volume
R^*	Critical radius (cm)
λ	Effective radius from Lindfors (cm)
ExpCorr	Exponential correction factor

Pre-exponential Term:

$$D_{mono} N_{Av} c^2 \left(\frac{k_B T}{\gamma}\right)^{1/2} \ln\left(\frac{c}{S}\right) \frac{R^*}{R^* + \lambda}$$

Exponential Term:

$$-ExpCorr \frac{16\pi}{3} \left(\frac{\gamma}{k_B T}\right)^3 \frac{v_m^2}{\ln\left(\frac{c}{S}\right)^2}$$

Biphasic Dissolution Model

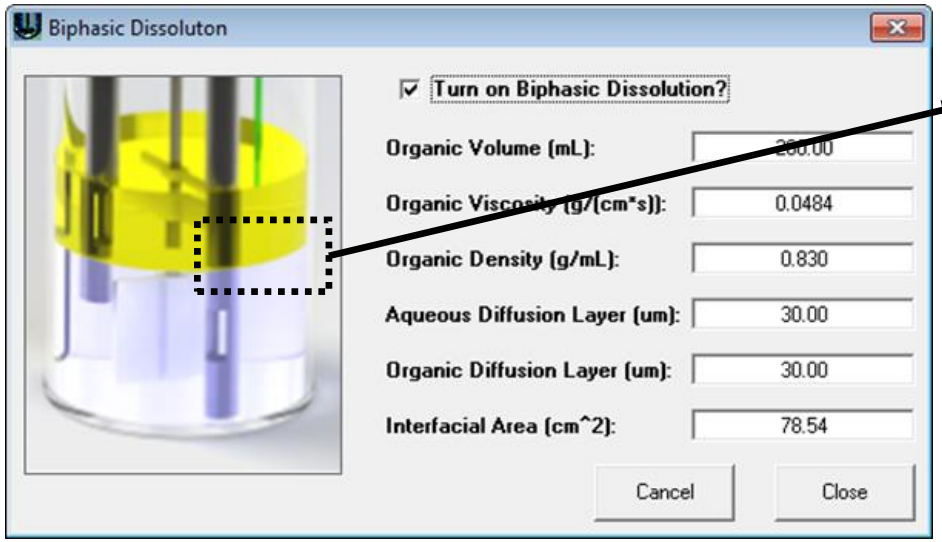

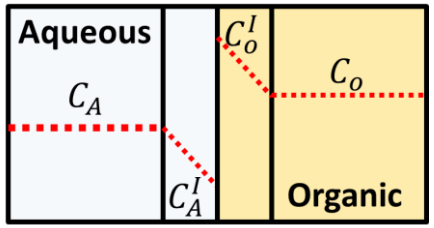

Itraconazole biphasic dissolution

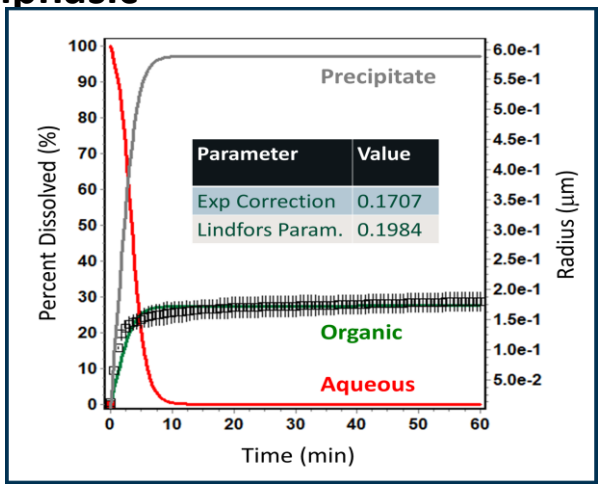

Mullin J. AAPS 2018, Poster W11230-05-037

Solution (**100 mg** Fasted)

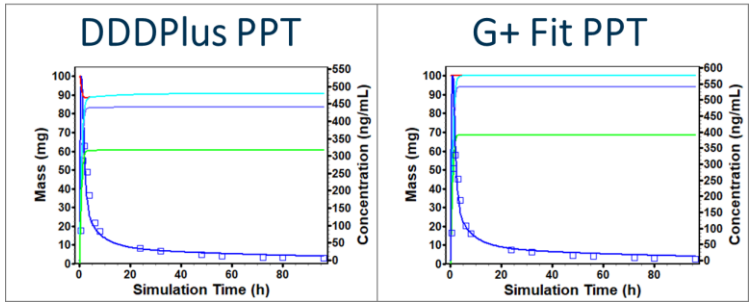

Capsule (**200 mg** Fasted)

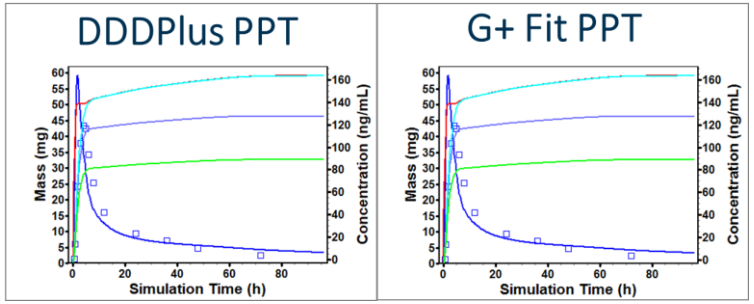

Solution (**200 mg** Fasted)

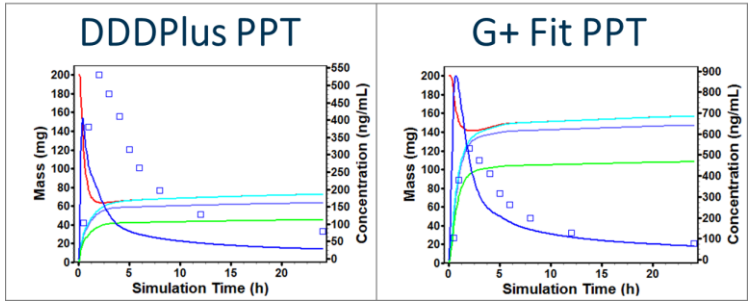

Capsule (**200 mg** fed)

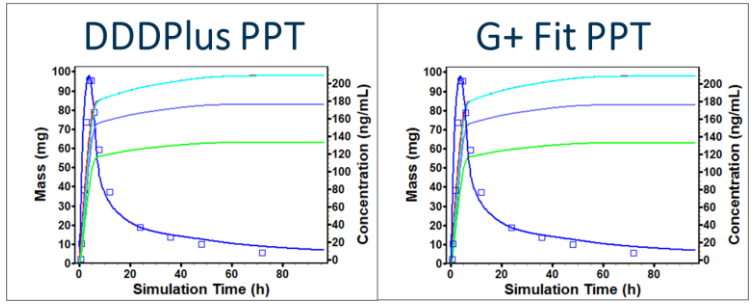

Solution (**200 mg** fed)

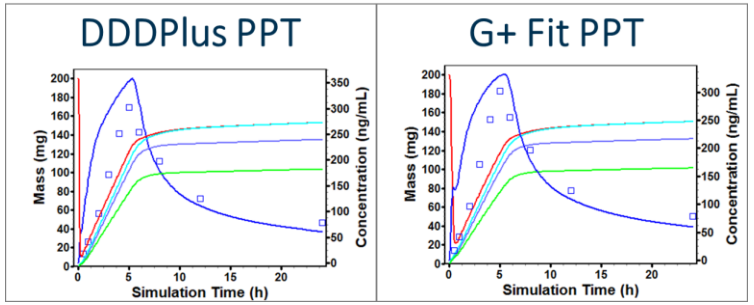

Amount Dissolved
Amount Portal Vein
Amount Absorbed
Total Entering Systemic Circ.
Cp Venous Return Predicted
Cp Venous Return Observed

Nimodipine

- **Physicochemical Properties**
- S+log P = 4.11 Exper. log P = 4.18
  (Biobyte Starlist)
- Aq. Sol (ug/mL) = 3.9 @ pH = 7.0
  (Yunzhe, Int. J. Pharmaceut., 2008)
- FaSSIF (ug/mL) = 12 @ pH = 6.5
  (Fu, Colloids Surf. B, 2013)
- S+Peff (cm/s x 10^4) = 1.77
  (AP 7.2)
- Caco-2 Papp (cm/s x 10^5) = 6.04
  (Agilent, Pub #5989-7668EN, 2007)
  - Converts to human jejunal Peff = 3.12 x 10^{-4} cm/s

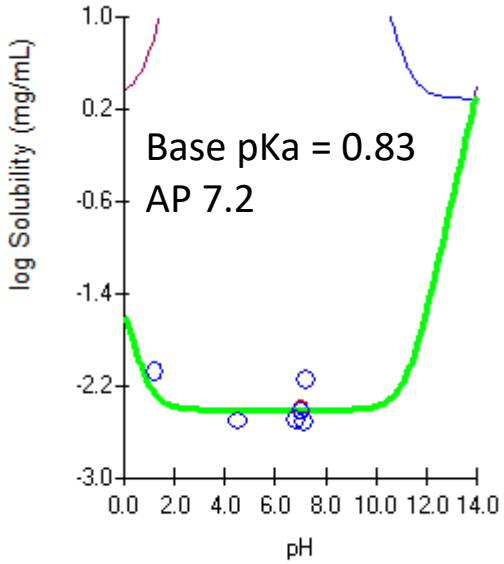

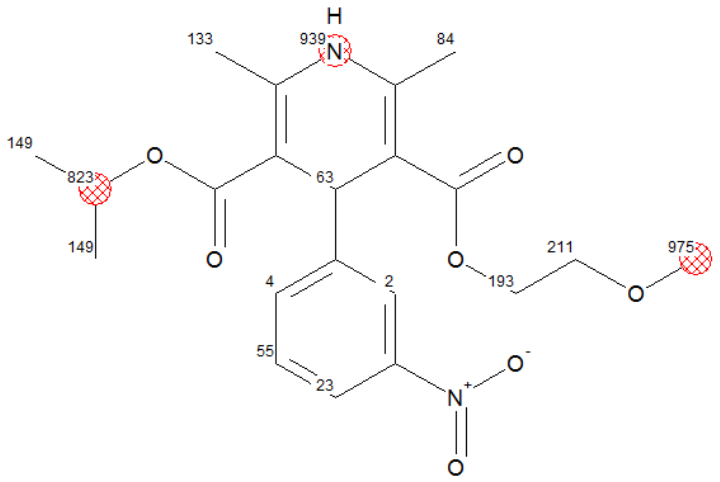

S+Predicted Sites of Metab. (CYP3A4)
S+3A4_K_m = 19 mM (AP 7.0)
S+3A4_V_{max} = 65.4 nmol/min/nmol Enz

AP 7.2 = ADMET Predictor 7.2, Simulations Plus, Inc.

Nimodipine Solid Dispersion

Amounts: red solid-dissolved, red dashed-precipitated, cyan-absorbed, blue-enteric portal vein, green-entering systemic circulation; Dark blue line and points – plasma concentration

1st order precipitation

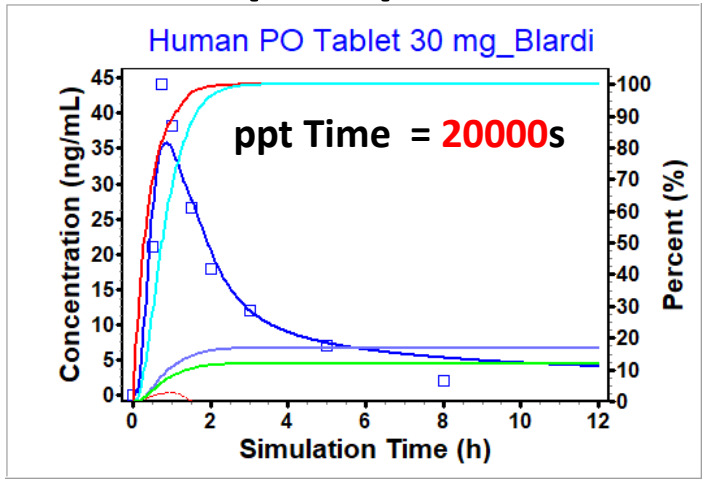

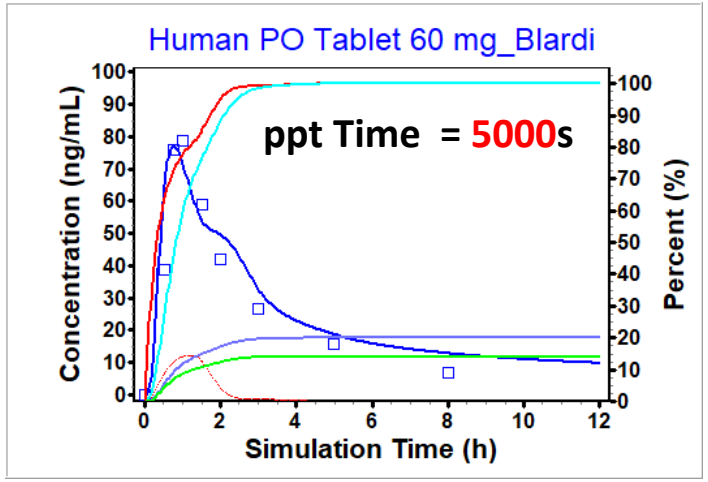

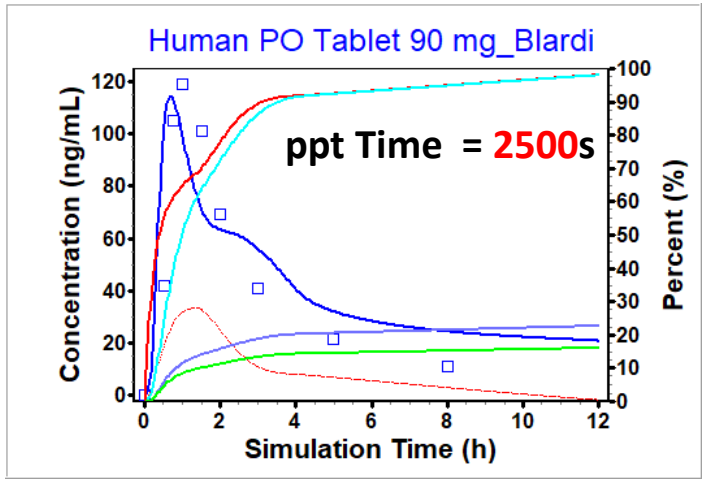

Mechanistic nucleation

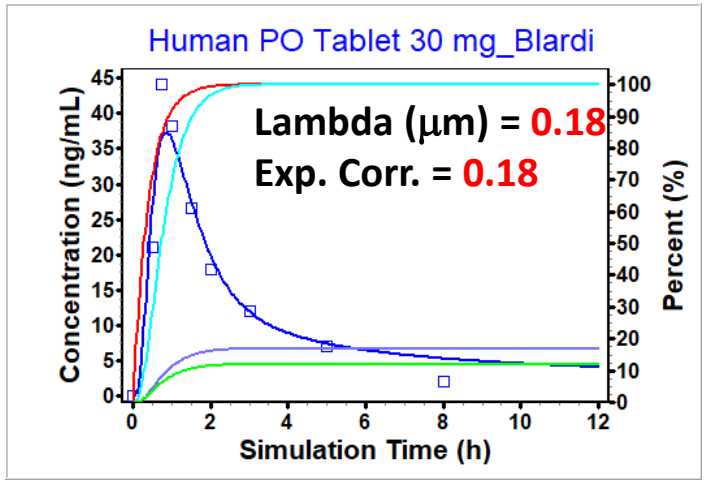

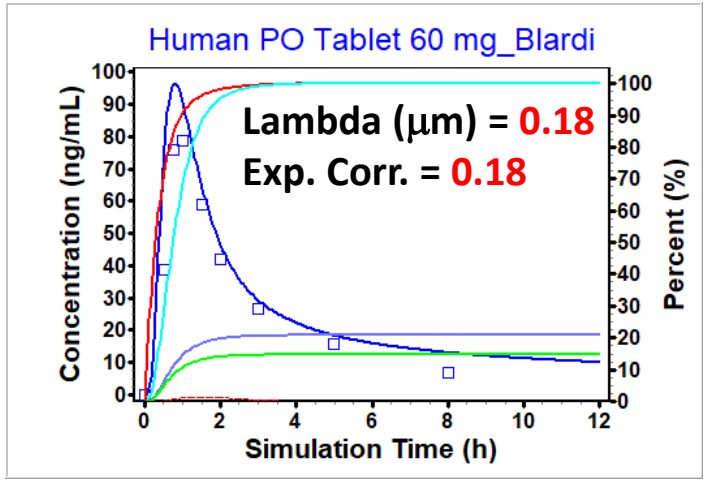

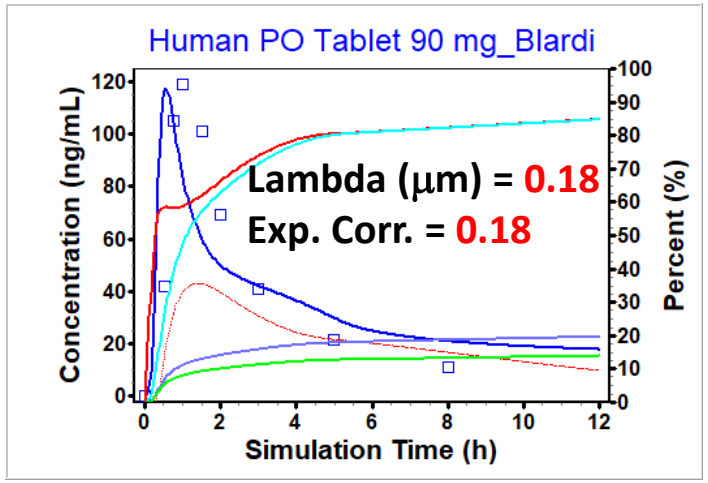

Absorption

Absorption Processes

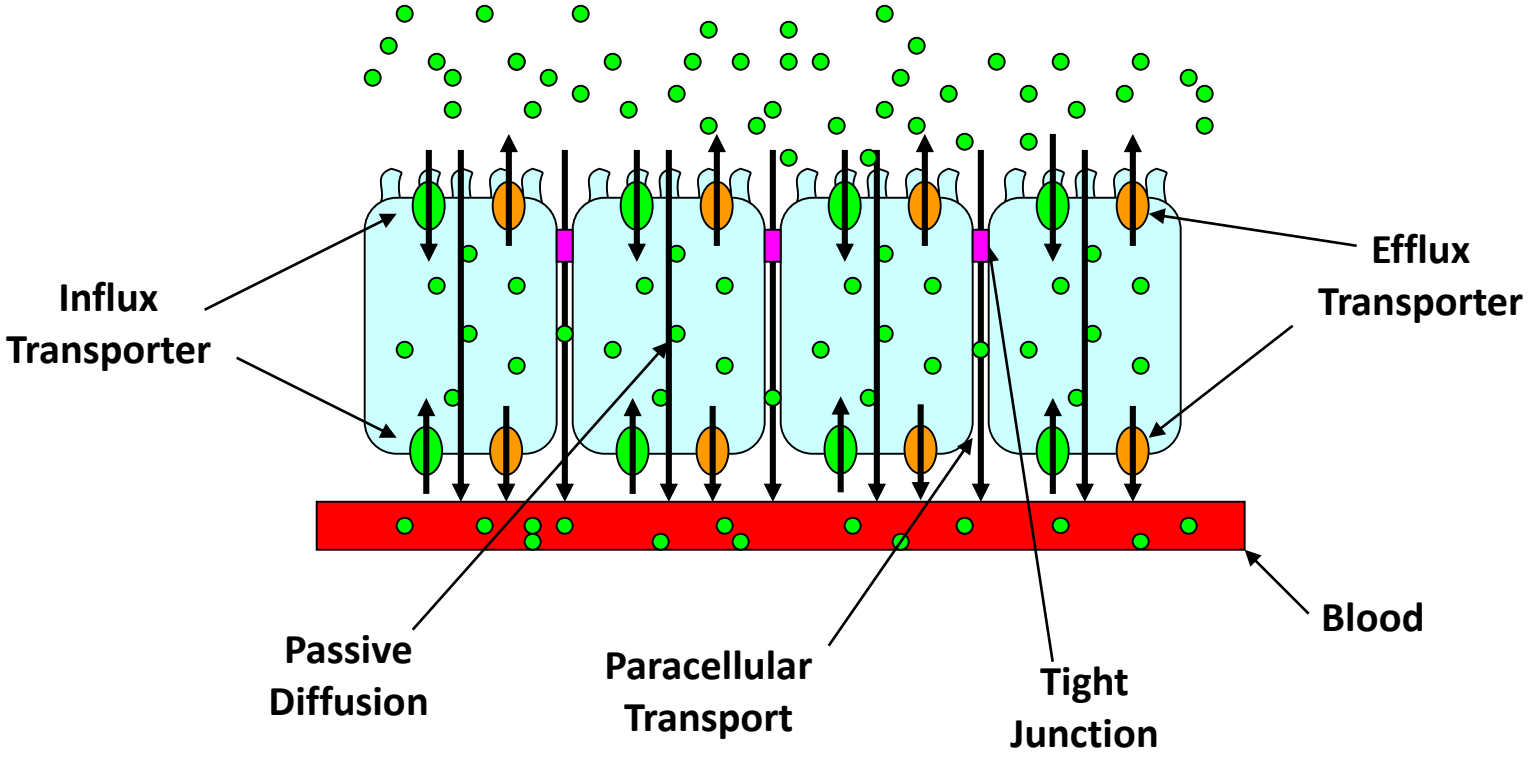

Effective Permeability (Peff): Measurements in Human

- Measure *disappearance* of drug from donor side
- Factors affecting permeability:
  - individual subject variations
  - adsorption to the tubes

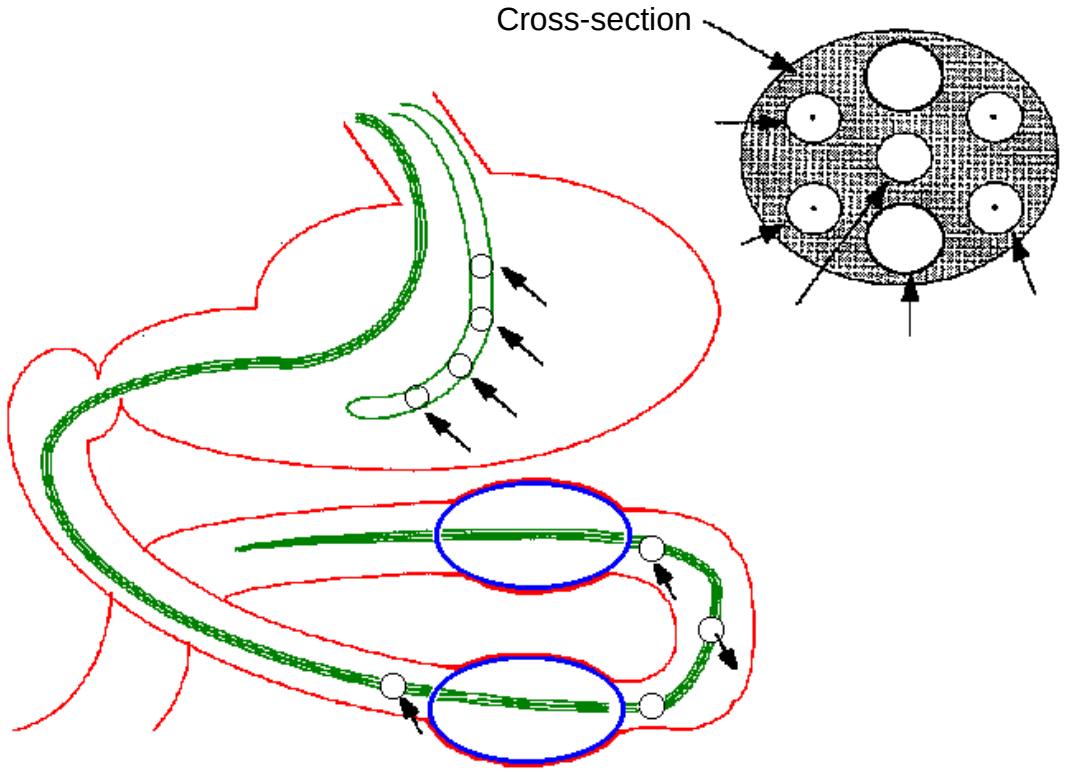

Peff = Q(Cin - Cout) /(2 π r L Cin)

r=1.75 cm, L=10 cm

Peff = 0.0091*Q(Cin - Cout) /Cin

H. Lennernas, G.L. Amidon, et al.Capsugel Library, 1995

in vitro Permeability (Papp) Experiments

- Measure *appearance* of drug on receiver side
- Many factors affect *in vitro* permeability (P_{app}):
  - pH on each side of the membrane
  - solvents (e.g., DMSO)
  - amount of protein on receiver side
  - concentration in donor side
  - shaking rate
  - nonspecific binding to plasticware

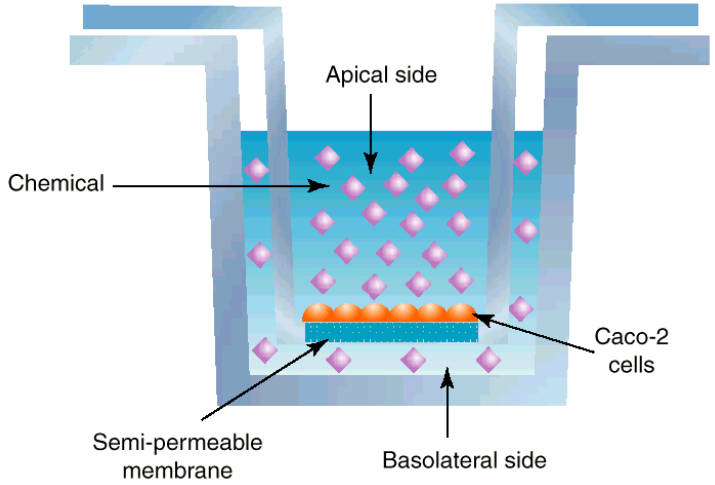

Li, A.P., DDT, 6(7):339-348

PAMPA Papp values for selected drugs collected from literature
All data are for Lecithin solution in dodecane and pH=7.4

Blue – Zhu Ch. EurJMedChem 2002, 37:399; Red – Ruell J.A. pION; Yellow – Kerns E.H. JPharmSci 2004, 93:1440; Green – Avdeef A. EurJPharmSci 2001, 14:271; Grey – Du C. pION

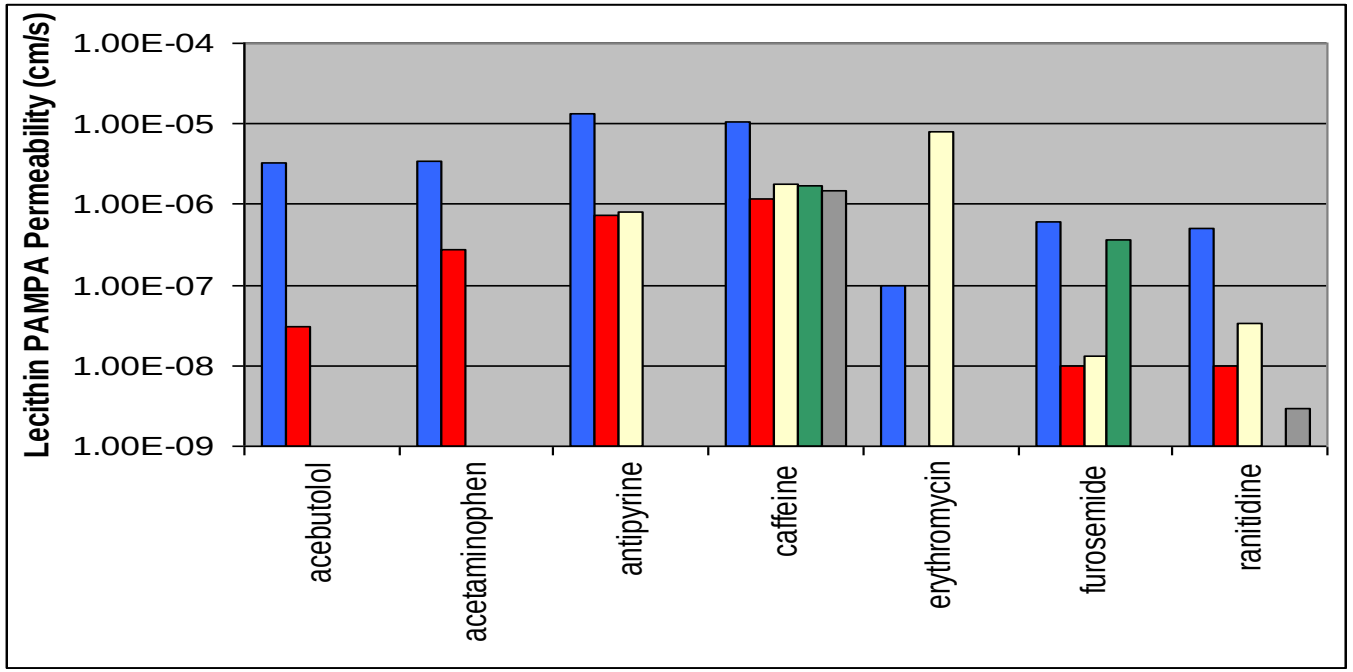

Mechanistic Simulations of *in vitro* Permeability (Papp) Experiments May Help with *in vitro/in vivo* Translation

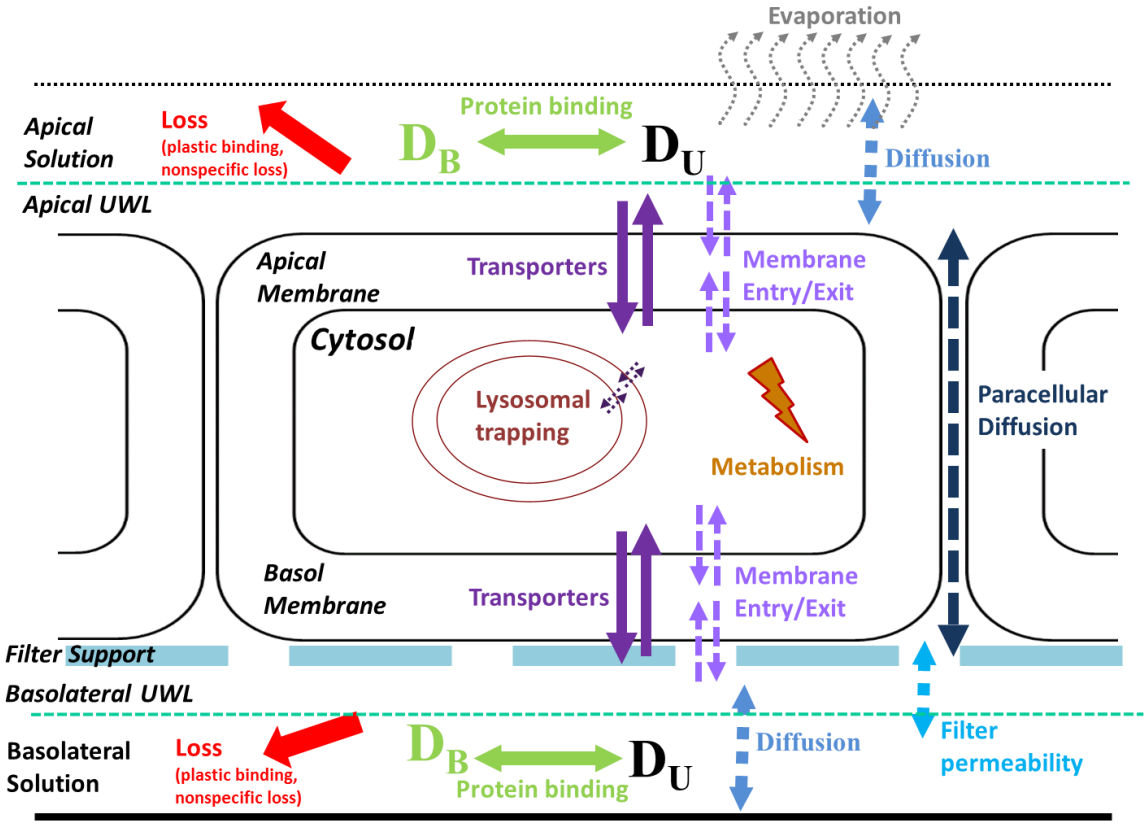

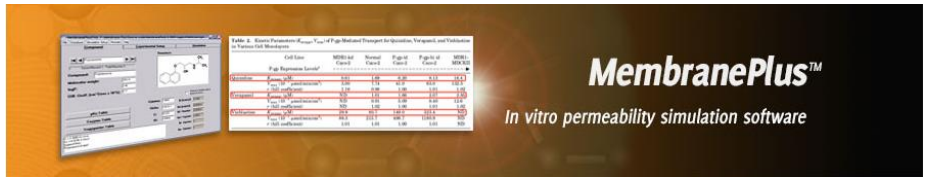

- Unlock important information related to absorption
- Number of different processes affecting apparent *in vitro* permeability can be included in the simulation:
  - Passive transcellular diffusion
  - Passive paracellular diffusion
  - Carrier mediated influx and/or efflux
  - Metabolism in the cells
  - Binding to albumin
  - Accumulation in cell membranes or intracellular compartments
  - Experimental conditions (e.g., shaking rate, pH)

MembranePlus™ Simulation for Methylphenidate

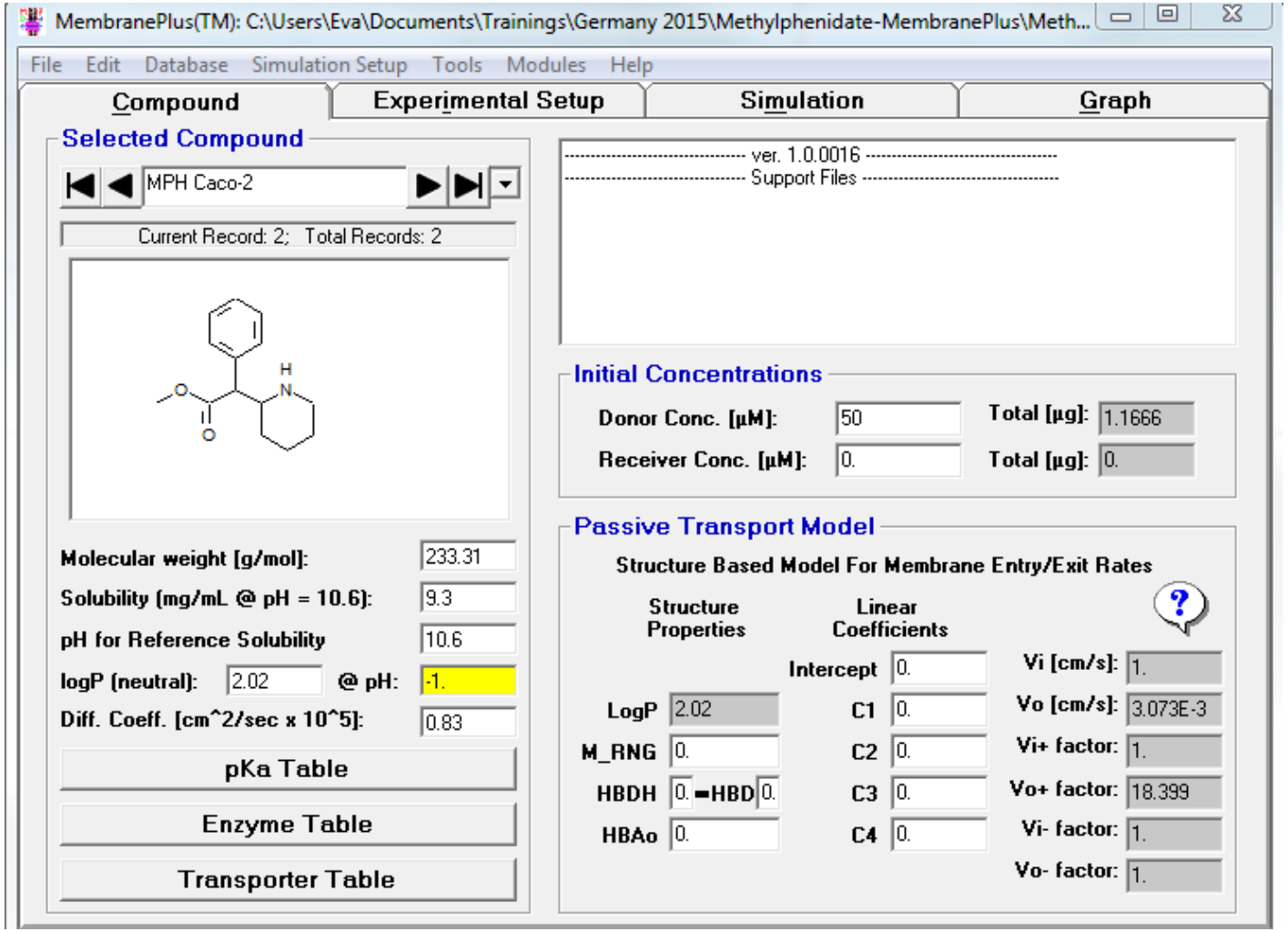

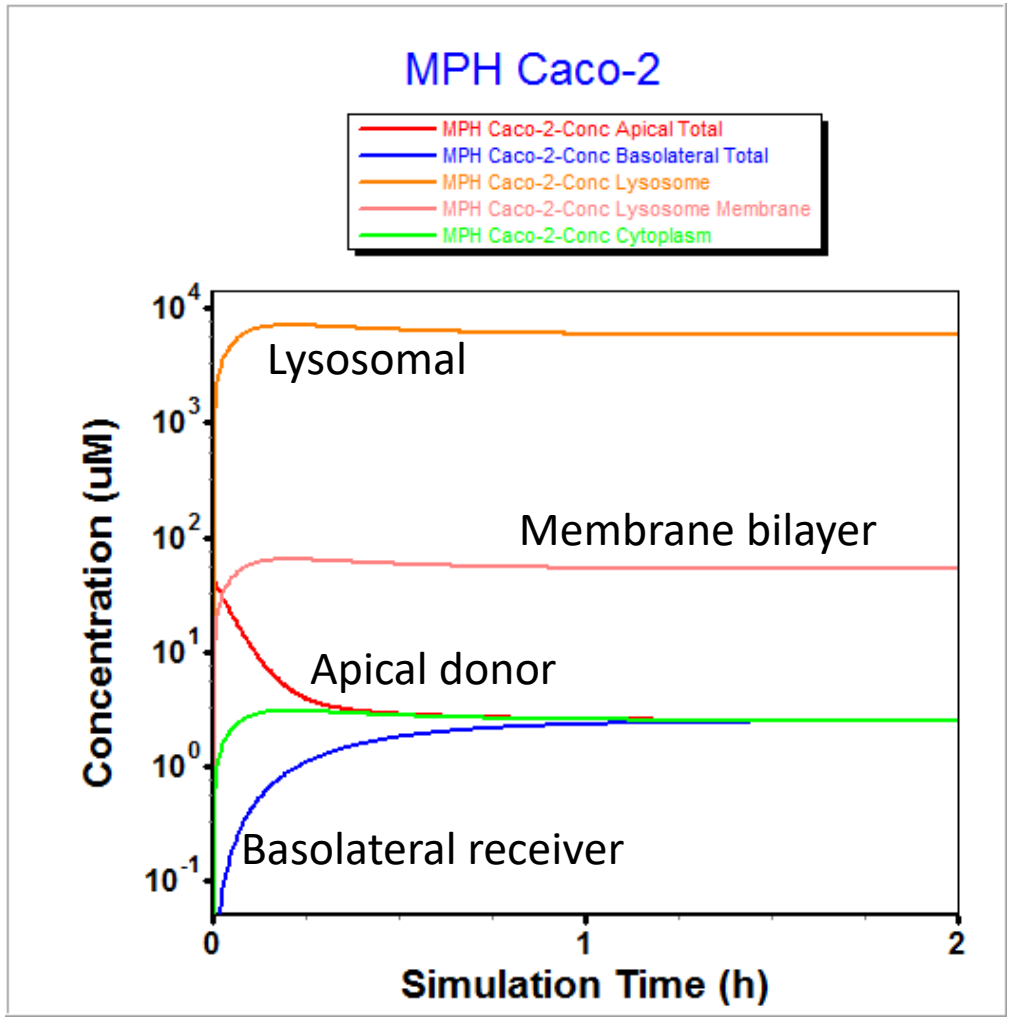

S+pKa = 8.56 (Base) (AP 7.2)

Nonlinear Processes

Metabolic Clearance

Step 1. *In vitro* incubation of drug with microsomes/hepatocytes/liver slices to obtain enzyme kinetic constants V_{max} and K_m and the *in vitro* intrinsic clearance

↓

Step 2. Scale *in vitro* enzyme kinetic constants to *in vivo* conditions based on species-specific physiological scale factors.

↓

Step 3. Based on a tissue blood flow model (e.g. Venous equilibrium model), determine *in vivo* hepatic clearance. Rate of drug elimination = CL_h × Concentration

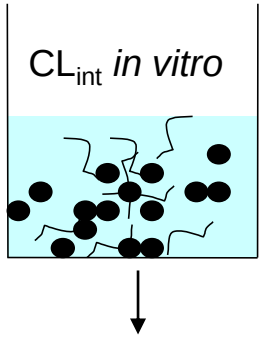

CL_{int} (whole organ) *in vitro*

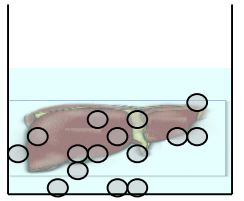

CL_h (whole organ) *in vivo*

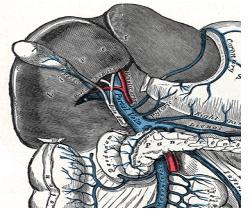

Houston and Carlile, Drug Metab. Rev. 29(4):891 (1997)

Midazolam Clearance IVIVE

Experimental			GastroPlus Compartmental Simulated				
Dose	Cmax	AUC	Cmax	AUC	Fa%	FDP%	Fb%
7.5	0.028	69	0.021	65	99	45	24
15	0.056	154	0.052	158	99	55	29
30	0.13	453	0.120	369	99	64	34

GastroPlus simulations of nonlinear dose dependence for midazolam using *in vitro* K_m and V_{max} and *iv* PK.
(Agoram et al., 2001)

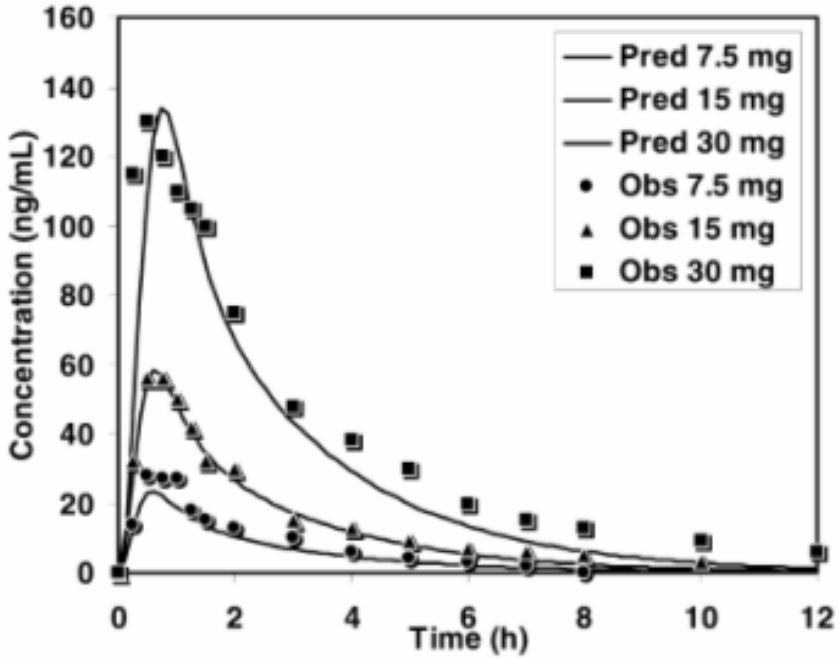

Transporter IVIVE – System Specific Scaling Factors

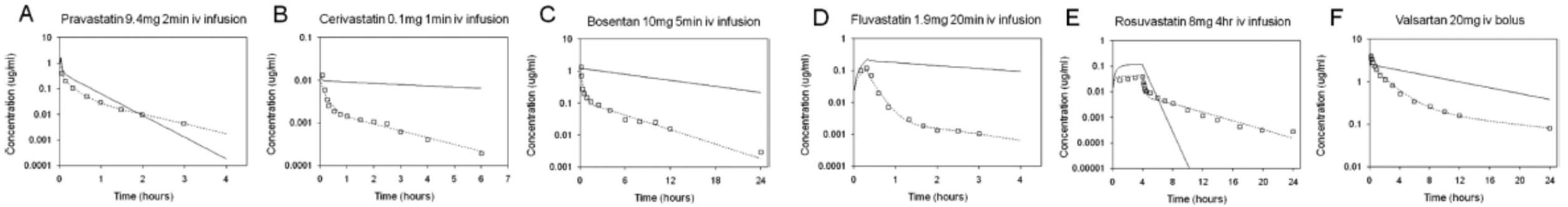

In vitro scaled and fitted sandwich culture human hepatocyte estimates

Compound	$SCL_{int,u,act}$			$SCL_{int,u,pass}$			$SCL_{int,u,bile}$		
	In Vitro-Scaled	In Vivo-Fitted	Scaling Factor	In Vitro-Scaled	In Vivo-Fitted	Scaling Factor	In Vitro-Scaled	In Vivo-Fitted	Scaling Factor
					l/h				
Pravastatin	19	406	21	1.1	4.2	3.9	12	1.5	0.12
Cerivastatin	102	12,827	126	265	153	0.58	182[a]	55[a]	
Bosentan	96	8489	89	51	59	1.2	165[a]	21[a]	
Fluvastatin	475	76,513	161	208	147	0.71	485[a]	86[a]	
Rosuvastatin	98	1190	12	18	1.7	0.10	16	1.2	0.079
Valsartan	22	2463	110	6.4	23	3.7	1017	25	0.024
Repaglinide	319	13,941	44	938	1477	1.6	0	0	
Geometric mean			58			1.0			0.061

[a] Represents the sum of $SCL_{int,u,bile}$ and $SCL_{int,u,met}$ because for these three compounds both CL mechanisms are occurring and they cannot be uniquely identified in the fitting process.

Solid lines – predicted from *in vitro* data;
Dotted lines – fitted to *in vivo* data

Jones et al., DMD 2012

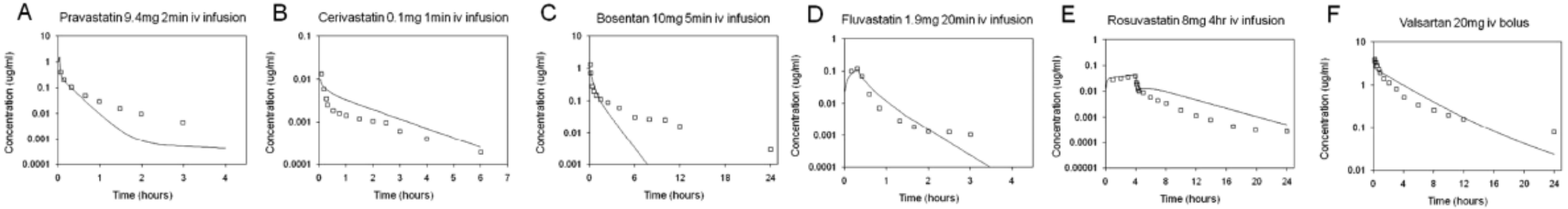

Transporter IVIVE – Compound Specific Scaling Factors

Rat

Human

prediction from *in vitro*

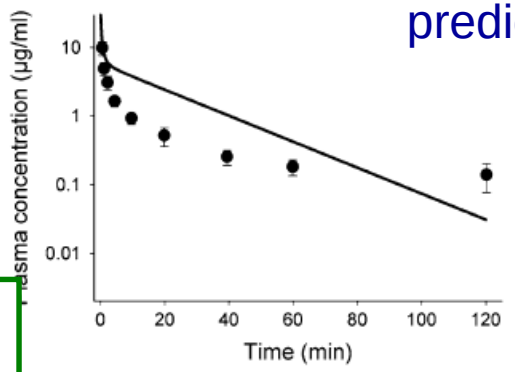

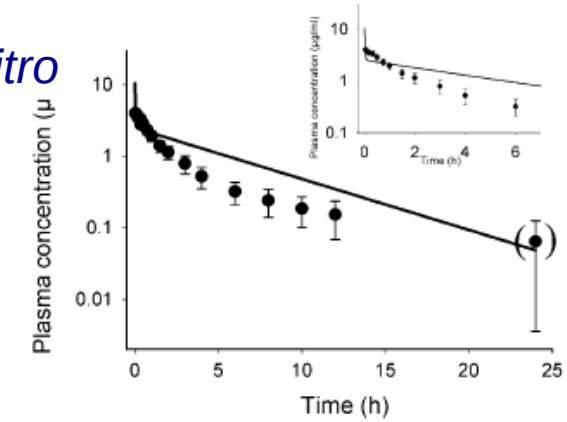

Use animal data to fit the empirical scaling factor

prediction with additional scaling factor

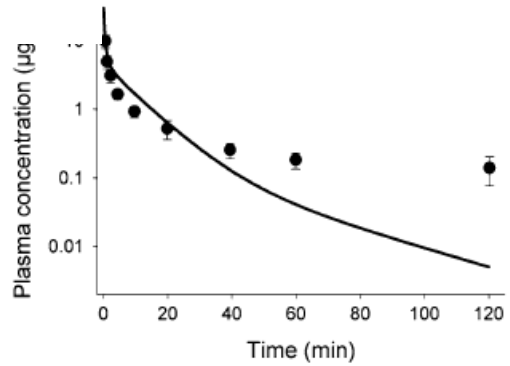

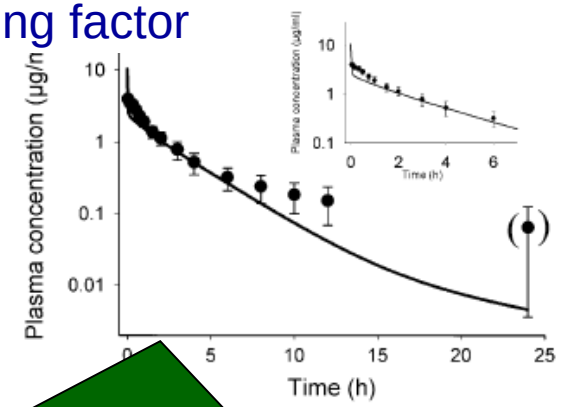

Apply the scaling factor from preclinical data to predict human PK

Poirier et al., J Pharmacokinet Pharmacodyn 2009

Transporter IVIVE – Scaling of Passive Diffusion Across Tissues

Hepatocytes transport data[a]	Wistar rats ($n = 3$) Mean ± SD	Cryopreserved human hepatocytes lot 77 Mean ± SD
Uptake from plasma (in vitro data)		
$K_{mI,u}$		
(μM)	28.4 ± 3.7	44.4 ± 14.6
(mg/l eq. μg/ml)	12.4 ± 1.6	19.3 ± 6.4
V_{maxI} (pmol/mg/min)	1318 ± 176	304 ± 85
J_{maxI} (mg/s)	0.0126 ± 0.0017	0.241 ± .067
P_{dif} (μl/mg/min)	1.21 ± 0.42	0.724 ± 0.271
PS_{TC} (ml/s)	0.0266 ± 0.0092	1.72 ± 0.49
f_b (%)	0.394 ± 0.171	0.417 ± 0.226
Excretion from liver to bile		
$K_{mE,u}$ (μg/g eq. mg/l	12.4	19.3
J_{maxE} (mg/s)	0.0126	0.241
PS_{TC} (ml/s)	0	

(Poirier – J Pharmacokinet Pharmacodyn 2009, 36:585)

Instead of empirical scaling factors
Include PStc scaling across tissues

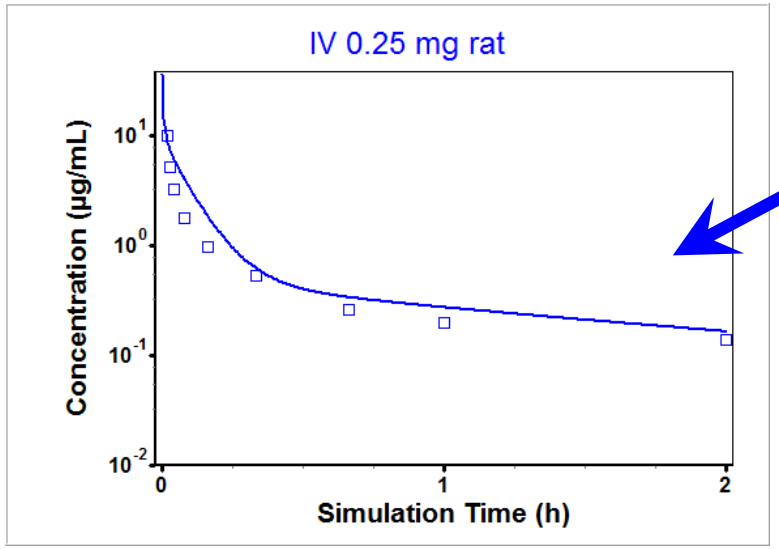

Apply the same approach
for human prediction

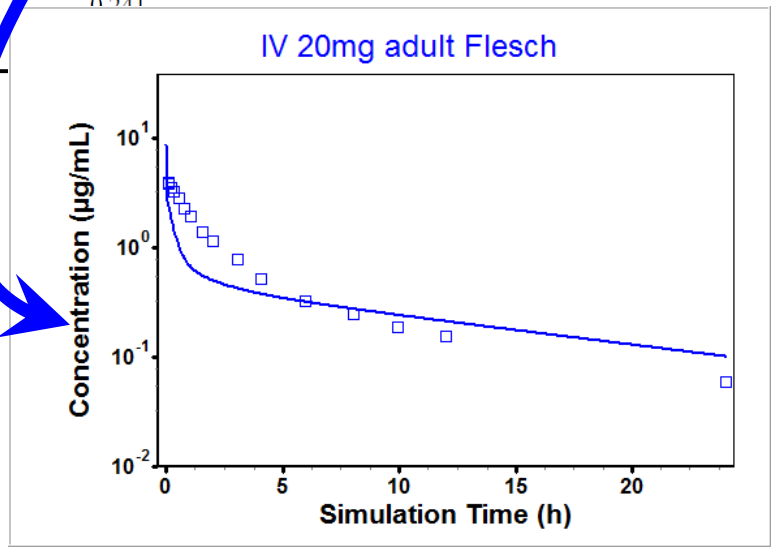

Lukacova – 17th North American ISSX meeting 2011, Atlanta, GA

IVIVE for efflux of digoxin – determining intracellular unbound Km

The intracellular unbound P-gp K_m for digoxin was found to be 95.3 mM by fitting B->A Papp with MembranePlus across experiments run at eight different concentrations and validated in a separate experiment using kinetic data at five concentrations

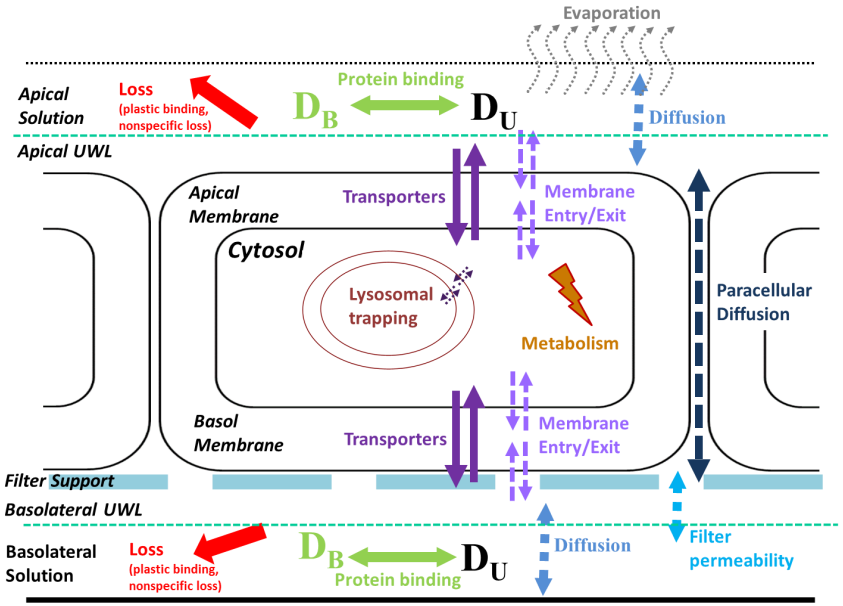

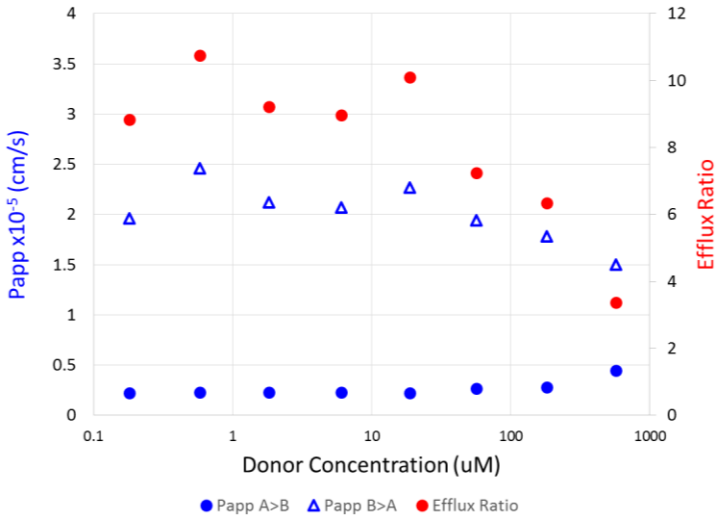

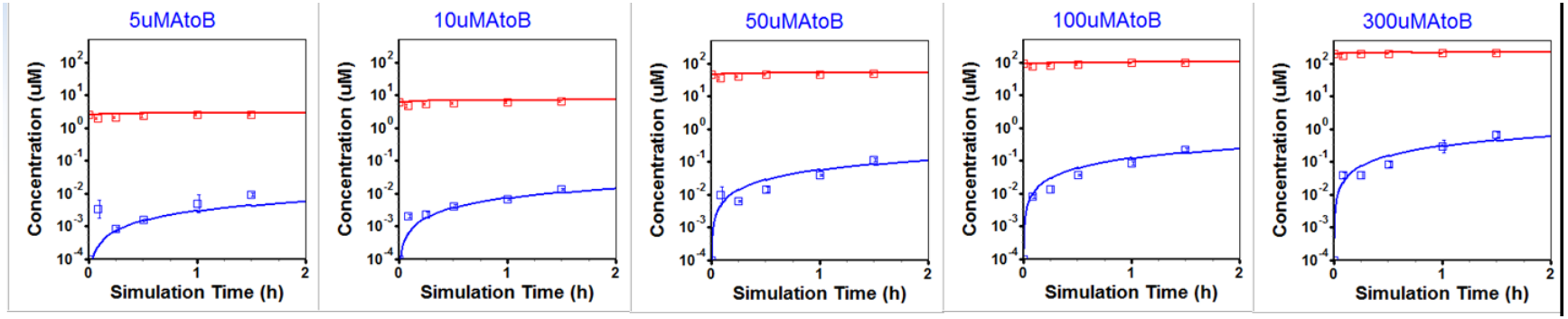

IVIVE for efflux of digoxin – predicting *in vivo* absorption

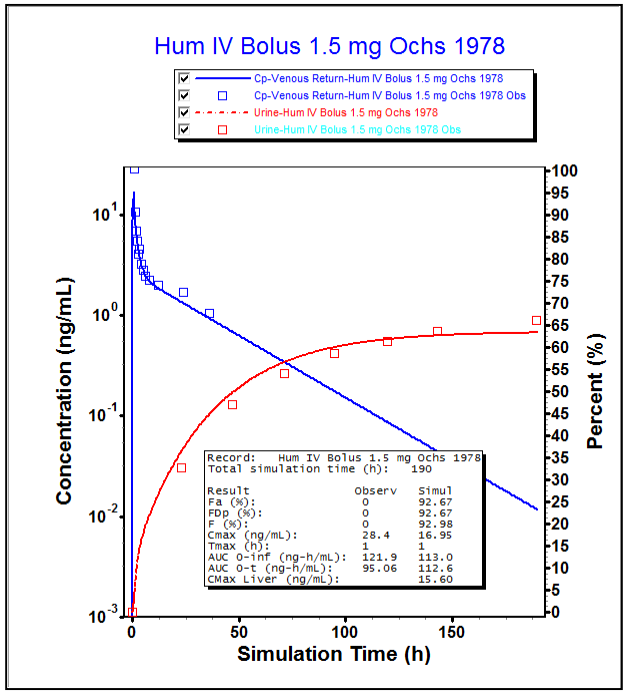

A

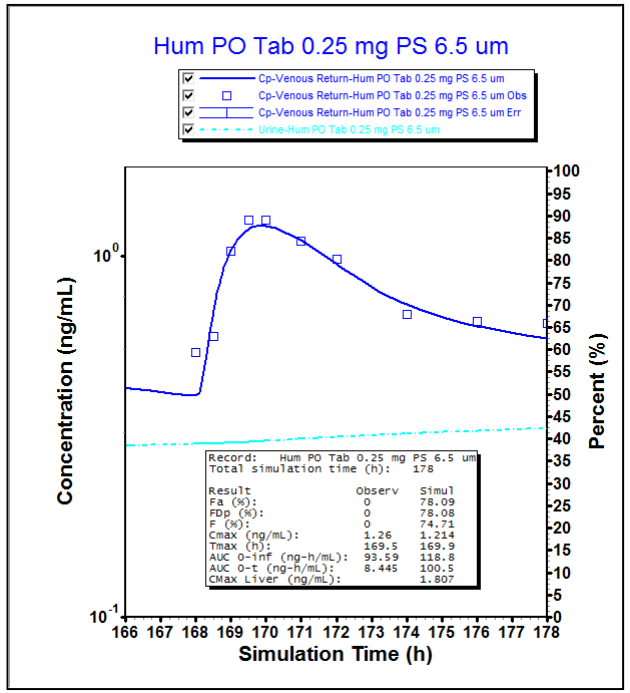

B

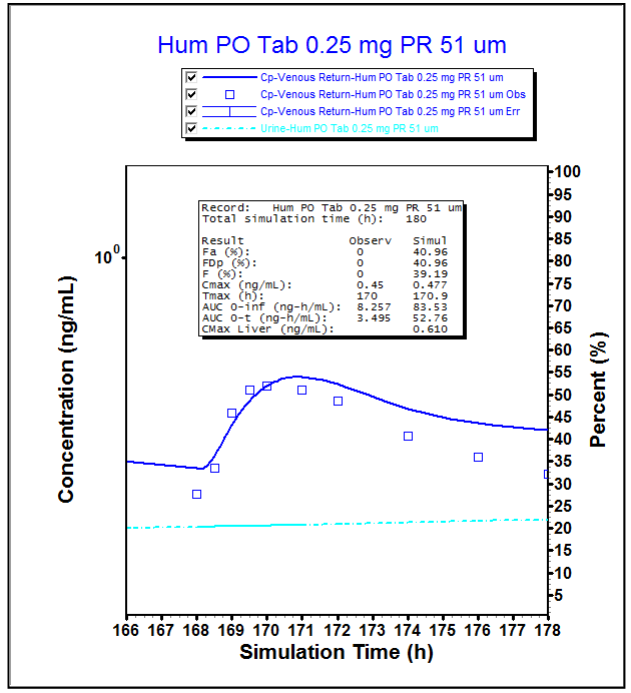

C

A: Observed (symbols) vs. predicted plasma conc. (blue) and urinary excretion (red) of digoxin (Ochs, 1978).
B: Observed (symbols) vs. predicted plasma conc. (blue) of digoxin for a PO formulation with 6.5 mm radius particle size (Jounela, 1975).
C: Observed (symbols) vs. predicted plasma conc. (blue) of digoxin for a PO formulation with 51 mm radius particle size (Jounela, 1975).

All simulations are using the fitted intracellular unbound P-gp Km value of 95.3 mM

Virtual Trials

Use Calibrated PBPK Model to: Predict Drug Behavior in Different Populations: Disease State

Pharmacokinetics of buspirone and its metabolite was predicted in patients by accounting for known physiological changes between healthy subjects and patients with liver cirrhosis:

- While the exposure for buspirone increased significantly (left) in decompensated liver cirrhosis, only minor changes were predicted for the 1-pyrimidinylpiperazine metabolite (right).
- Both sets of simulations are in reasonable agreement with observed data (blue points).
- Simulations in both groups of subjects are for 10mg tablet

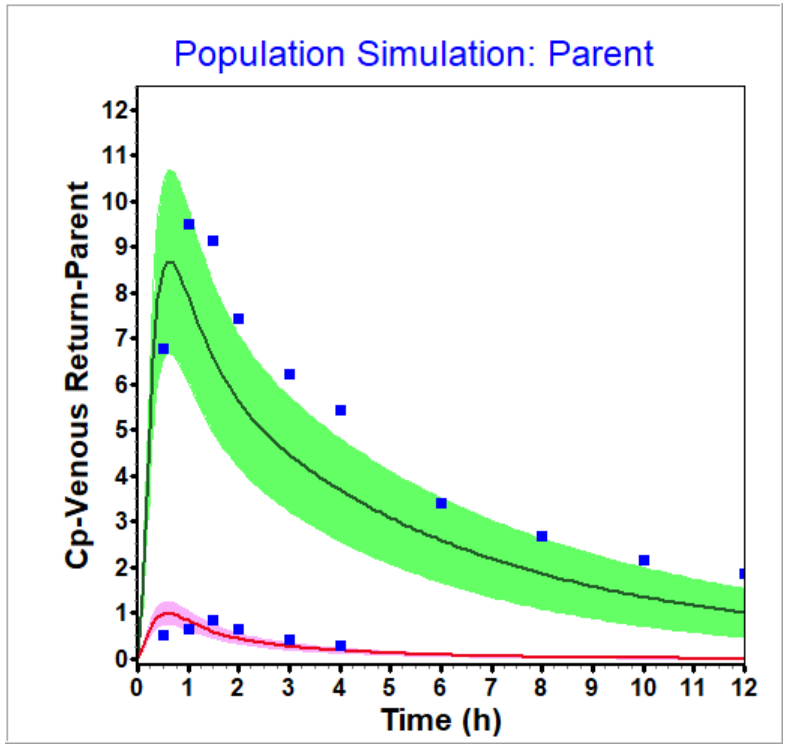

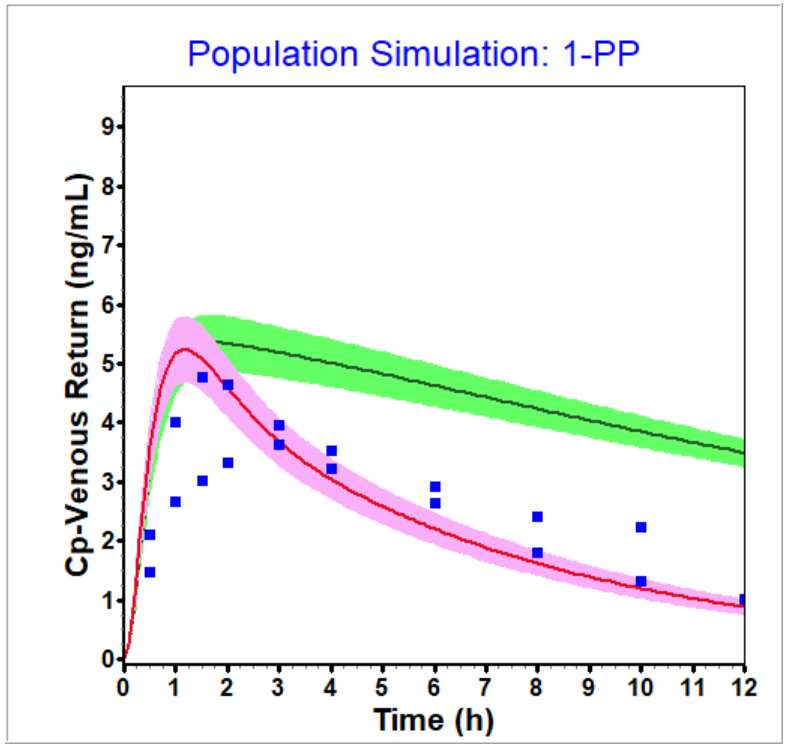

green – simulation result in patients with cirrhosis;
pink – simulation result in healthy subjects

Baseline model described in Macwan J., Poster presentation ACoP 2014

Use Calibrated PBPK Model to: Predict Drug Behavior in Different Populations: Pediatric

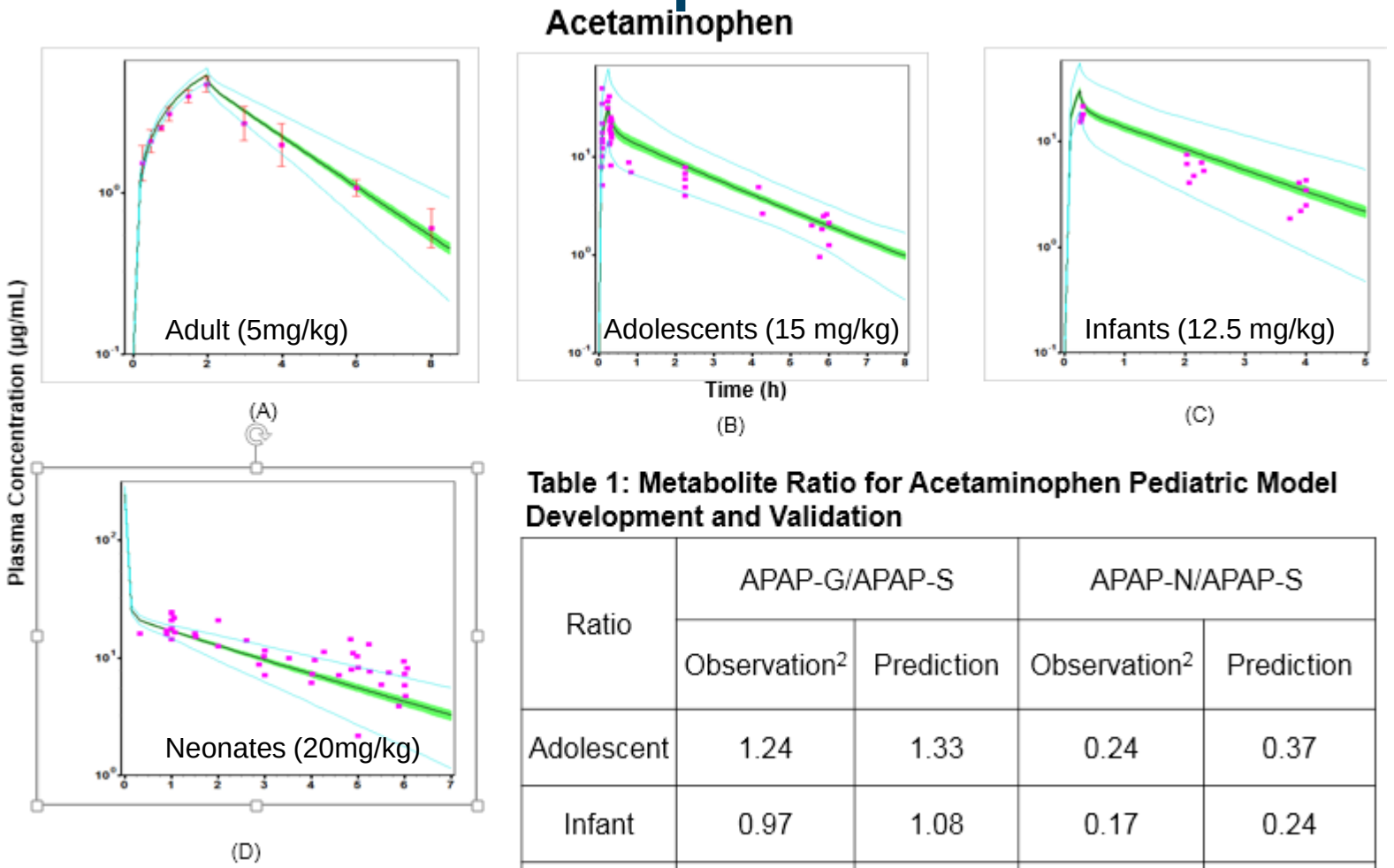

Table 1: Metabolite Ratio for Acetaminophen Pediatric Model Development and Validation

Ratio	APAP-G/APAP-S		APAP-N/APAP-S	
	Observation[2]	Prediction	Observation[2]	Prediction
Adolescent	1.24	1.33	0.24	0.37
Infant	0.97	1.08	0.17	0.24
Neonate	0.60	0.71	0.12	0.08

Samant et al. – Poster Presentation (Poster # 111) - ASCPT 2015
also Quantitative Systems Pharmacology pre-conference Poster # QP-16

Use Calibrated PBPK Model to: Compare Formulations by Accounting for Variability

Incorporate measured variability for physicochemical, formulation, physiology and PK parameters into Population Simulator

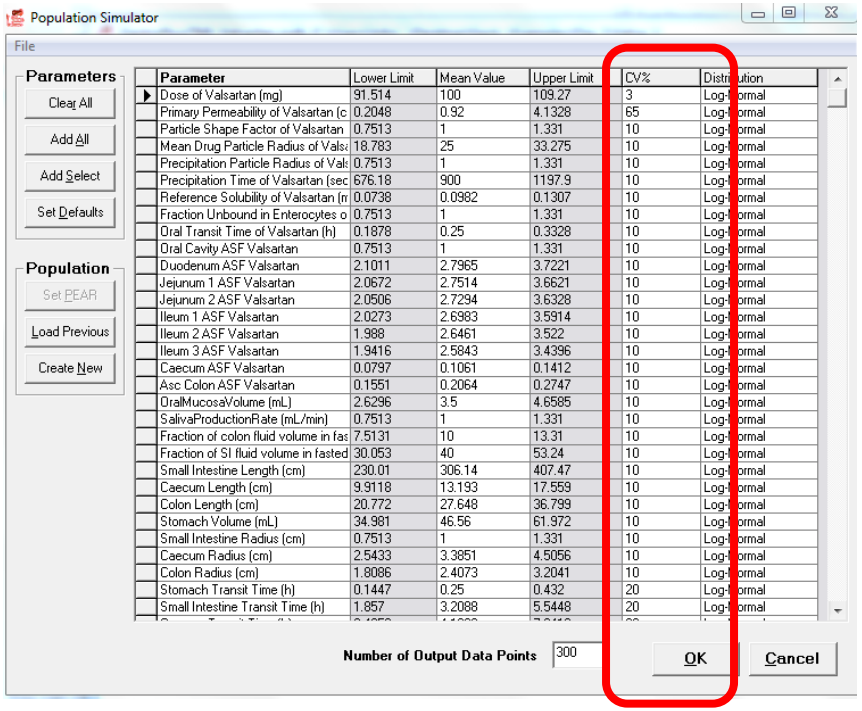

Tistaert, C. AAPS Annual Meeting 2015, Orlando, FL

Capture observed variability from existing clinical PK studies

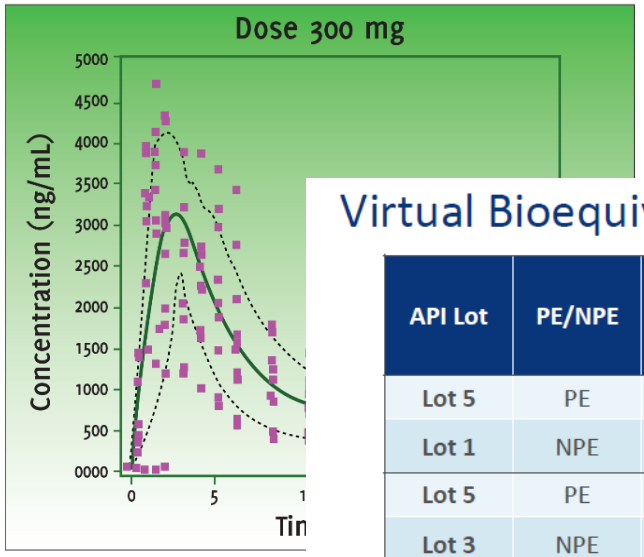

Virtual Bioequivalence Study Simulations

API Lot	PE/NPE	Dose (mg)	AUC_{∞} (ng.h/mL) (N=250)		C_{max} (ng/mL) (N=250)		
			GM	GMR (90% CI)	GM	GMR (90% CI)	
Lot 5	PE	50	4180	113.3 (110.7, 116.1)	551	139.3 (136.0, 142.7)	≠
Lot 1	NPE	50	3688		395		
Lot 5	PE	100	8242	103.0 (100.9, 105.1)	551	106.4 (104.3, 108.6)	=
Lot 3	NPE	100	8001		395		
Lot 5	PE	300	24998	102.2 (99.8, 104.6)	3118	100.0 (97.7, 102.4)	=
Lot 2	NPE	300	24460		3117		
Lot 5	PE	100	8242	98.2 (96.2, 100.2)	1068	95.1 (93.2, 97.0)	=
Lot 4	NPE	100	8395		1123		
Lot 5	PE	300	24998	101.9 (99.8, 104.1)	3118	98.3 (96.3, 100.4)	=
Lot 4	NPE	300	24525		3171		

API: active pharmaceutical ingredient; AUC_{∞}: area under the plasma concentration-time curve from time 0 to infinite time; CI: confidence interval; C_{max}: maximum observed plasma concentration; GM: geometric mean; GMR: geometric mean ration; NPE: non-particle-engineered; PE: particle-engineered

Use Calibrated PBPK Model to: Establish Dissolution Specifications for a Formulation

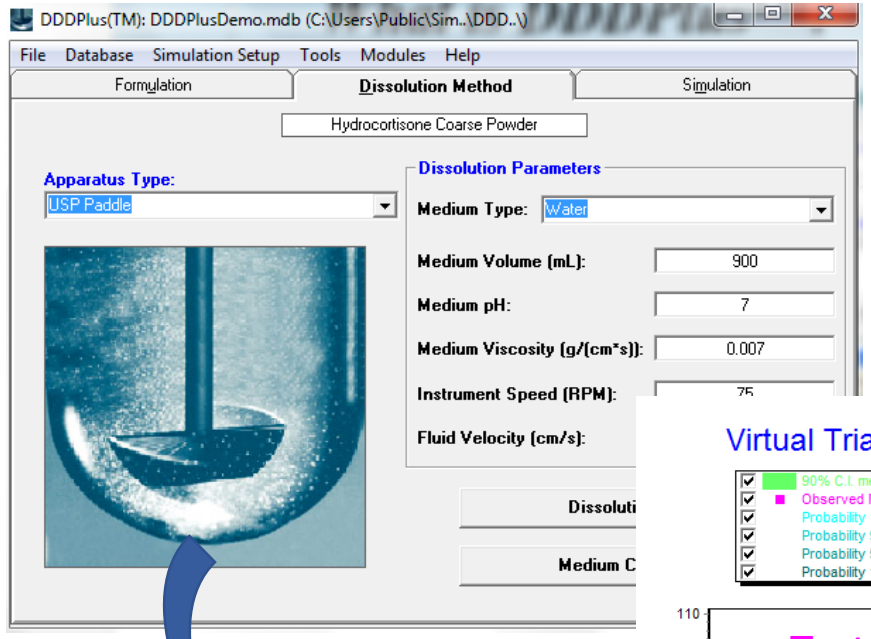

Mechanistic *in vitro* simulation may be used to estimate expected variability in *in vitro* dissolution

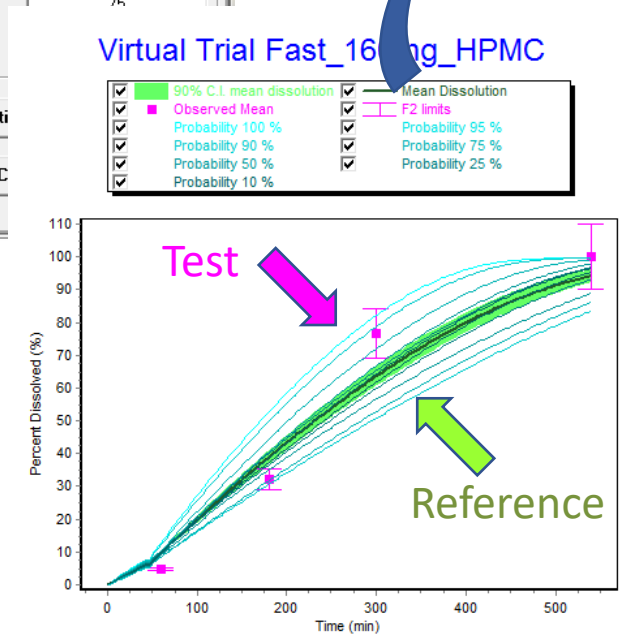

PBPK model will be used to evaluate whether the variability *in vitro* is likely to translate into significant differences in *in vivo* performance

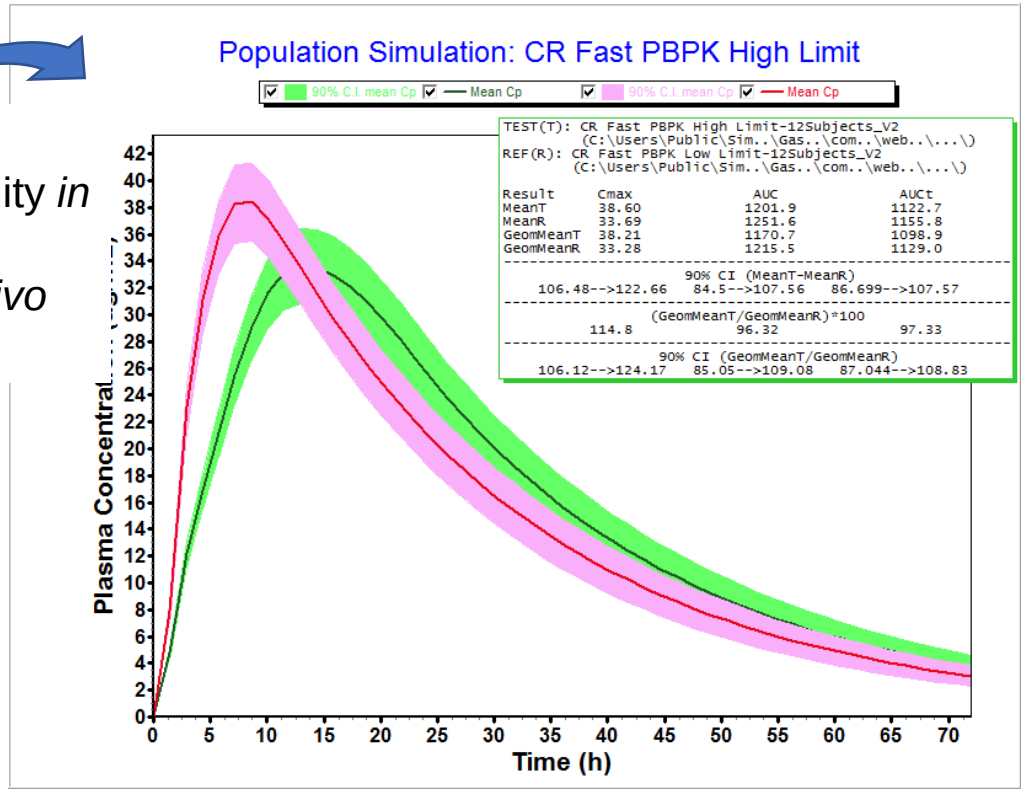

Summary

- PBPK models allow incorporating different types of *in vitro* measurements into single platform to account for all processes affecting drug's absorption, distribution and elimination.
- Confidence in predictions of *in vivo* behavior based on *in vitro* data still varies between processes due to gaps in physiology characterizations, adequate *in vitro* assays, or lack of validation examples.
- Mechanistic simulations of *in vitro* assays can be used to 'deconvolute' important parameter values and aid in *in vitro* – *in vivo* extrapolation of different processes.
- PBPK models linked with information on population differences and physiological variability allow for prediction of variability in population of subjects, prediction of drug behavior between different groups of subjects, comparison of different formulations.

Questions

Contact: viera@simulations-plus.com

Or visit: www.simulations-plus.com

SimulationsPlus

SCIENCE + SOFTWARE = SUCCESS